NATIONAL ADVISORY COMMITTEE FOR AERONAUTICS

TECHNICAL NOTE

No. 1759

EFFECTS OF COMPRESSIBILITY ON NORMAL-FORCE, PRESSURE, AND LOAD CHARACTERISTICS OF A TAPERED WING OF NACA 66-SERIES AIRFOIL SECTIONS WITH SPLIT FLAPS

By F. E. West, Jr., and J. M. Hallissy, Jr.

Langley Aeronautical Laboratory
Langley Field, Va.

Washington

December 1948

NATIONAL ADVISORY COMMITTEE FOR AERONAUTICS

TECHNICAL NOTE NO. 1759

EFFECTS OF COMPRESSIBILITY ON NORMAL-FORCE, PRESSURE, AND LOAD CHARACTERISTICS OF A TAPERED WING OF NACA 66-SERIES AIRFOIL SECTIONS WITH SPLIT FLAPS

By F. E. West, Jr., and J. M. Hallissy, Jr.

SUMMARY

A high-speed wind-tunnel investigation of a tapered wing of NACA 66-series airfoil sections equipped with split flaps has been conducted at Mach numbers up to 0.585 to determine the effects of compressibility on the normal-force, pressure, and load characteristics. Both 55-percent-span and 98-percent-span flaps deflected 60° and having chords of 20 percent of the wing chord were tested. The range of angle of attack investigated was from approximately -4° up through the stall.

The maximum normal-force curves for the wing with flaps were somewhat similar in shape to the maximum lift curve for the wing without flaps, although Mach number effects became apparent at lower speeds and were larger for the wing with flaps. The maximum normal-force coefficient for the wing with partial-span split flaps reached a minimum value of 1.53 at a Mach number of 0.295 and a maximum value of 1.79 at a Mach number of 0.585. The maximum normal-force coefficient for the wing with full-span split flaps reached a minimum value of 1.87 at a Mach number of 0.300 and a maximum value of 2.22 at a Mach number of 0.550. There is further evidence that the rapid rise in maximum lift coefficient at higher Mach numbers is due to the sharp leading edge of the wing as camber, camber location, and trailing-edge angle appear to have little or no effect on the rise.

Mach number has a very slight effect on the shift of lateral center of normal force for angles of attack below the stall.

INTRODUCTION

Until recently only scattered results have been obtained from wind-tunnel tests (references 1 and 2) and from flight tests (references 3 and 4) on the effects of both Reynolds and Mach numbers on the maximum-lift characteristics of airfoils. These tests indicated the importance of a more extensive knowledge of these effects on the maximum lift coefficient both in the estimation of the maneuvering performance and loads of high-speed aircraft and in the interpretation of wind-tunnel

maximum-lift data as applied to the prediction of airplane characteristics at low speeds. Hence, an investigation of a series of typical fighter-type wings has been undertaken in the Langley 16-foot high-speed tunnel and in the Langley 19-foot pressure tunnel. The primary purpose of the investigation in the Langley 16-foot high-speed tunnel has been to study the effect of Mach number on maximum-lift characteristics up to a Mach number of approximately 0.60, and in the Langley 19-foot pressure tunnel, the primary purpose has been to study the interrelated effects of Mach number and Reynolds number on maximum lift characteristics up to a Mach number of approximately 0.35.

The first wing in the series to be investigated had a 12-foot span, NACA 230-series airfoil sections with thickness ratios decreasing linearly from 16 percent at the root to 9 percent at the tip, a taper ratio of 2:1, and an aspect ratio of 6. The results of the investigation in the Langley 16-foot high-speed tunnel are presented in references 5 and 6, and the results of the investigation in the Langley 19-foot pressure tunnel are presented in reference 7.

The second wing in the series to be investigated had a plan form similar to the first wing and was composed of 16-percent-thick NACA 66-series airfoil sections. The results of the plain-wing investigation in the Langley 16-foot high-speed tunnel are presented in references 8 and 9. These results indicate an increasing maximum lift coefficient from a Mach number of 0.15 to a peak value at a Mach number of 0.25, then a rapid decrease from a Mach number of 0.25 to 0.35 and a lower rate of decrease from a Mach number of 0.35 to 0.50, and then a rapid rise from a Mach number of 0.50 to 0.60.

In order to determine the variation of maximum lift coefficient with Mach number for the wing with split flaps, tests were conducted of this wing equipped with both partial- and full-span flaps at flap angles of 60°. This paper presents the results of these tests which were made in the Langley 16-foot high-speed tunnel. However, as only pressure data were obtained, normal-force coefficients are presented instead of lift coefficients. The variation of normal-force coefficient with either Mach number or angle of attack is assumed to be indicative of the variation of lift coefficient with either Mach number or angle of attack.

In addition to the normal-force characteristics, representative span-load distributions, lateral centers of normal force, pitching-moment coefficients, flap normal-force and hinge-moment coefficients, and chordwise pressure distributions are also presented.

SYMBOLS

Free-stream conditions:

V_o corrected airspeed, feet per second

a_o speed of sound in air, feet per second

M_o	Mach number (V_o/a_o)
M_{cr}	Mach number at which speed of sound is attained locally at some point on wing
ρ_o	mass density of air, slugs per cubic foot
q_o	dynamic pressure, pounds per square foot $\left(\frac{1}{2}\rho_o V_o^2\right)$
p_o	static pressure, pounds per square foot
μ_o	coefficient of viscosity of air, slugs per foot–second
R_o	Reynolds number $(\rho_o \bar{c} V_o/\mu_o)$

Wing geometry:

S	wing area, square feet
b	wing span, feet
A	aspect ratio (b^2/S)
$\bar{c}$	mean geometric chord, feet (S/b)
c	airfoil chord at any spanwise station, feet
c'	mean aerodynamic chord, feet $\left(\frac{2}{S}\int_0^{b/2} c^2 dy\right)$
x	chordwise distance measured from airfoil leading edge, feet
y	spanwise distance measured from plane of symmetry of wing, feet
α	corrected angle of attack of wing at plane of symmetry, degrees

Force data:

L	wing lift, pounds
C_L	wing lift coefficient $(L/q_o S)$

Pressure data:

p local static pressure, pounds per square foot

P pressure coefficient $\left(\frac{p - p_o}{q_o}\right)$

P_{cr} pressure coefficient corresponding to local Mach number of 1

c_n wing section normal-force coefficient $\left(\int_0^1 (P_L - P_U)\, d\left(\frac{x}{c}\right)\right)$

$c_n \frac{c}{\bar{c}}$ section load parameter

C_N wing normal-force coefficient $\left(\int_0^1 c_n \frac{c}{\bar{c}}\, d\left(\frac{y}{b/2}\right)\right)$

c_{n_f} flap section normal-force coefficient $\left(\int_0^1 \left(P_{L_f} - P_{U_f}\right)\, d\left(\frac{x_f}{c_f}\right)\right)$

C_{N_f} flap normal-force coefficient $\left(\int_0^1 c_{n_f} \frac{c_f}{\bar{c}_f}\, d\left(\frac{y_f}{b_f/2}\right)\right)$

$\frac{y_{cp}}{b/2}$ position of lateral center of normal force, fraction of semispan $\left(\frac{\int_0^1 c_n \frac{c}{\bar{c}} \frac{y}{b/2}\, d\left(\frac{y}{b/2}\right)}{\int_0^1 c_n \frac{c}{\bar{c}}\, d\left(\frac{y}{b/2}\right)}\right)$

x_l distance from leading edge of each spanwise station to line perpendicular to plane of symmetry and passing through 25-percent position of mean aerodynamic chord, feet

$c_{m_{x_l}}$ section pitching-moment coefficient due to force acting perpendicular to chord line about a line perpendicular to plane of symmetry and passing through 25-percent position of mean aerodynamic chord $\left(\int_0^1 (P_L - P_U) \left(\frac{x_l}{c} - \frac{x}{c}\right) d\left(\frac{x}{c}\right)\right)$

$c_{m_{x_1}}\left(\frac{c}{\bar{c}}\right)^2$ section pitching-moment parameter due to force acting perpendicular to chord line

$C_{m_{c'/4}}$ pitching-moment coefficient about 25-percent position of mean aerodynamic chord

$$\left(\left[\frac{\bar{c}}{c'}\int_0^{1.0} c_{m_{x_1}}\left(\frac{c}{\bar{c}}\right)^2 d\left(\frac{y}{b/2}\right)\right] + C_{N_f}\sin\theta\,\frac{S_f}{S}\,\frac{z}{c'}\right)$$

θ included angle between wing and flap chords

z distance measured from flap center of pressure perpendicular to mean aerodynamic chord

c_{h_f} flap section hinge-moment coefficient

$$\left(\int_0^1 \left(P_{L_f} - P_{U_f}\right)\left(\frac{-x_f}{c_f}\right)\, d\left(\frac{x_f}{c_f}\right)\right)$$

$c_{h_f}\left(\frac{c_f}{\bar{c}_f}\right)^2$ flap section hinge-moment parameter

C_{h_f} flap hinge-moment coefficient $\left(\int_0^{1.0} c_{h_f}\left(\frac{c_f}{\bar{c}_f}\right)^2 d\left(\frac{y}{b_f/2}\right)\right)$

Subscripts:

f flap

L lower surface

U upper surface

i incompressible

c compressible

max maximum

MODEL AND INSTALLATION

The wing, equipped with both partial- and full-span split flaps, mounted in the Langley 16-foot high-speed tunnel for the pressure tests is shown in figures 1 and 2. The solid-steel wing was made to conform to the airfoil ordinates given in table I. The split flaps were constructed of $\frac{3}{16}$-inch steel plate and were attached to the wing by $\frac{5}{8}$-inch steel

blocks. Glazing putty was used to insure an airtight seal at the junction of the flaps and wing.

A diagrammatic sketch of the wing is given in figure 3. The principal dimensions of the wing and flaps given in this figure are also included with other pertinent information in the following table:

Wing span, feet	12
Wing area, square feet	24
Aspect ratio	6
Taper ratio	2:1
Mean aerodynamic chord, feet	2.07
Root section:	
Airfoil section	NACA 66 series (a = 0.6)
Design lift coefficient	0.1
Thickness–chord ratio	0.16
Tip section:	
Airfoil section	NACA 66 series (a = 0.6)
Design lift coefficient	0.2
Thickness–chord ratio	0.16
Sweepback (along leading edge), degrees	6.34
Dihedral (along quarter–chord line), degrees	0
Geometric twist (washout), degrees	1.55
Flap span:	
Partial–span flaps, percent wing span	98
Full–span flaps, percent wing span	55
Flap chord, percent wing chord	20
Flap angle (included angle between wing lower surface and flap), degrees	60

In the left semispan of the wing, 35 wing and 7 flap pressure orifices were distributed over each of six spanwise stations. (See fig. 3.) The wing pressure tubes were brought through a steel tube mounted rigidly to the wing, and the flap pressure tubes were run along the back of the flaps to a hole in the boom used to conduct pressure tubes out of the wing. (See figs. 2 and 3.) All the tubes were conducted through the boom and then through a counterbalanced tail strut to multitube manometers.

The wing was mounted on shielded struts having a thickness–chord ratio of 0.15. The thickness–chord ratio of the shields was 0.124.

A cathetometer was used to determine changes in angle of attack due to distortion in the support or scale system by measuring variations in the height of marks scribed below the wing surface on the left–wing support struts.

TESTS

For approximate Mach numbers of 0.20, 0.30, 0.40, and 0.50, pressure data for both flap configurations were obtained for a range of angle of attack from approximately -4° up through the stall. For other Mach numbers from 0.145 to 0.585 pressure data were obtained over a range of angle of attack sufficient to define the stall. Power limitations prevented obtaining maximum normal force above a Mach number of 0.550 for the full-span flap configuration and above a Mach number of 0.585 for the partial-span flap configuration.

Most of the tests were run by maintaining a constant indicated tunnel Mach number and by varying the angle of attack. A few tests were run by varying the tunnel speed and by maintaining a constant angle of attack for the full-span flap configuration because the wing pitching mechanism lacked sufficient power to change angle of attack above a Mach number of 0.50. The variation of test Reynolds number with Mach number is given in figure 4. Inasmuch as the various investigations were made during different seasons, the curves in figure 4 do not agree because of the change of prevailing temperatures.

CORRECTIONS

No attempt was made to correct individual pressure readings because no adequate method is available for calculating wind-tunnel-wall effects on individual pressure readings. All pressure-test results were based on a tunnel-empty calibration.

Neither corrections due to the effect of the tunnel walls on the span-load distributions nor blockage corrections have been applied to the data. An investigation of the blockage corrections indicated a maximum normal-force-coefficient correction of 2 percent and a maximum Mach number correction of 1 percent.

The angle of attack has been corrected for support-system deflection, air-stream misalinement, and tunnel-wall effects. Results of tests of the wing without flaps gave an air-stream-misalinement value of approximately 0.2° upflow, which was used for the present investigation. The angle of attack was corrected for tunnel-wall effects by the methods of reference 5 except that the correction due to induced curvature of the flow was altered to apply to a wing with flaps.

RESULTS AND DISCUSSION

In order to show the effect of flaps on the characteristics of the wing, a large number of the results for the wing without flaps are presented

in this paper. Most of these results have been obtained or determined from the figures of reference 8.

Normal-Force Characteristics

The general normal-force and stalling characteristics of the three wing configurations are shown in figure 5.

Normal-force-curve slopes.- Upon exceeding the low-drag range, which occurs at an angle of attack of approximately $5\frac{1}{2}^\circ$, the slope of the normal-force curves for the wing without flaps decreases. This phenomenon is characteristic of a wing consisting of these airfoil sections and is discussed in reference 10. This decrease in normal-force-curve slope does not occur for the wing with either partial- or full-span flaps except for one test condition. The exception occurs for the wing with full-span flaps at a Mach number of 0.200. A careful check of the pressure distributions and of the test conditions does not reveal any reason for this apparent discrepancy.

Variation of normal-force coefficient with Mach number.- In order to obtain a better comparison of the variation of normal-force coefficient with Mach number for the three wing configurations, data from figure 5 are presented in figure 6 along with calculated curves based on a modification of the Glauert-Prandtl theory. (See reference 11.) This theory assumes low induced velocities over a wing and is, therefore, not directly applicable to a wing at high angles of attack or to a wing with flaps, but is used as a basis for the comparison of data. If a two-dimensional normal-force-curve slope of 2π is assumed, the calculated increase of normal-force coefficient with Mach number is

$$\frac{C_{N_c}}{C_{N_i}} = \frac{A + 2}{2 + A\sqrt{1 - M_o^2}}$$

Below the critical Mach number and for angles of attack of less than 8° the theory is applicable and good agreement is obtained with data for the plain wing (fig. 6(a)). For angles of attack above 8°, the experimental curves rise more rapidly with an increase in Mach number than do the calculated curves. The experimental curves also rise more rapidly through the complete angle-of-attack range for the wing with flaps.

Upon first exceeding the critical Mach number the normal-force coefficients for the wing without flaps show a decrease that is associated with the build-up of trailing-edge separation and the decrease of lower-surface pressures. Then at the high angles of attack as the Mach number is further increased these coefficients increase rapidly owing to the formation of extensive supersonic regions over the forward part of the upper surface. (See reference 8.) For the wing with flaps no decrease in the normal-force coefficients for moderate and high angles of attack occurs upon exceeding the critical Mach number. As can be seen in figure 7, which

shows the effect of Mach number on pressure distributions at a typical spanwise station, the pressures over the trailing edge and lower surface do not change enough upon exceeding the critical Mach number to cause a decrease in normal-force coefficient similar to that observed for the wing without flaps. With partial-span flaps a slight build-up of trailing-edge separation and a decrease in lower-surface pressures occur on the outboard sections of the wing at moderate and high angles of attack upon exceeding the critical Mach number; however, this does not have much effect on the wing normal-force coefficient because the outboard sections of the wing contribute a smaller part of the total wing normal force than the inboard sections.

At the high angles of attack the normal-force coefficients for the wing with flaps increase rapidly at the higher Mach numbers in a manner similar to that noted for the wing without flaps. In figure 7 it can be seen that for Mach numbers above 0.485 large supersonic regions extending over the forward part of the upper surface occur for the wing with flaps. This figure shows that as the Mach number is increased from 0.485 to 0.535, a well-established shock becomes evident along with a large increase in the area of the pressure distribution. As the Mach number is further increased to 0.550, the shock shifts toward the trailing edge and the extent of the supersonic region along the chord changes from approximately 25 to 33 percent of the chord. Thus, it is apparent that the increases in the normal-force coefficients at high Mach numbers and high angles of attack are due to the formation of large supersonic regions which cause large area increases in the pressure distributions.

Maximum normal-force coefficient.- The effect of Mach number on maximum normal-force coefficient for all three wing configurations and on maximum lift coefficient for the wing without flaps is shown in figure 8. The value of maximum lift coefficient for the wing without flaps increases with Mach number up to a low-speed peak value at a Mach number of approximately 0.25. The values of the maximum normal-force coefficients for the wing with partial- and full-span flaps increase with Mach number up to low-speed peak values at a Mach number of approximately 0.20. These increases in maximum lift coefficient and maximum normal-force coefficient are essentially a Reynolds number effect. Increasing the Reynolds number moves the transition point forward along the chord which gives the flow more resistance to separation. With an increase in Reynolds number, therefore, higher angles of attack and lift and normal-force coefficients can be reached before stalling occurs (reference 12). For the wing without flaps the maximum normal-force coefficient for Mach numbers below 0.30 is not typical of wings having NACA 66-series airfoil sections as indicated in reference 8. It is also believed that the maximum value occurring at a Mach number of 0.145 for the wing with full-span flaps should have been higher. Actually, the normal-force curves (fig. 5) for these conditions should reach higher peak values and should show a stall similar to the curve for a Mach number of 0.200 in figure 5(b). A wing consisting of these airfoil sections has a sensitive reaction to flow changes caused by variations

in surface conditions and although an effort was made to keep the wing clean at all times, the results at low Mach numbers were probably affected by surface conditions. Also, in the case of the wing alone, a difference in Reynolds number between force tests and pressure tests probably caused part of the difference between the maximum normal-force curve and the maximum lift curve at the lower Mach numbers. At higher Mach numbers, however, the normal-force curve and lift curve for the wing without flaps show much better agreement.

After the low-speed peak values of maximum normal-force coefficient are reached for the three wing configurations, the favorable effect of Reynolds number is counteracted by large adverse pressure gradients, back of the peak pressures, that tend to induce separation. Further increase in Mach number leads to the build-up of these adverse pressure gradients (reference 13) which finally induce separation from the leading edge.

Leading-edge separation causes a rapid loss of lift coefficient for the wing without flaps until a Mach number of approximately 0.32 is reached. Although the pressure peaks become more reduced above this Mach number, they also broaden due to the effect of Mach number. This change in the peaks tends to partly counteract the loss in lift coefficient, and the lift coefficient decreases at a slower rate until a minimum is reached at a Mach number of 0.50. The large increase in lift coefficient above this Mach number is due to the formation of extensive supersonic regions over the forward part of the upper surface similar to those shown in figure 7. A more complete discussion of maximum lift coefficient for the wing without flaps is presented in reference 8.

As the pressures are generally higher over the wing with flaps, the effects of Mach number on the maximum normal-force coefficients are larger and become apparent at lower speeds for the wing with flaps than for the wing without flaps. Thus, since large adverse pressure gradients that induce separation from the leading edge occur at lower Mach numbers for the wing with flaps, the low-speed peak values for these configurations are reached at lower Mach numbers. This separation also causes a larger loss and a more rapid decrease of normal-force coefficient for the wing with flaps than of lift coefficient for the wing without flaps. The effects of separation are largest for the wing with full-span flaps.

After this rapid decrease the normal-force coefficient does not change with an increase in Mach number for the wing with partial-span flaps. For the wing with full-span flaps the normal-force coefficient slowly increases. These conditions prevail because the pressure peaks change in a manner similar to those observed for the wing without flaps at a sufficiently fast rate to counteract or to more than counteract the loss in normal-force coefficient.

Above an approximate Mach number of 0.50, the normal-force coefficient for the flap configurations rises rapidly for the same reason as observed for the lift coefficient for the wing without flaps, namely the formation of large areas of supersonic flow.

The maximum-lift characteristics of the NACA 230-series wing discussed in reference 5 differ appreciably from those of the NACA 66-series wing. The maximum lift curve for the NACA 230-series wing reaches a low-speed peak value at a Mach number of approximately 0.30, after which it decreases steadily with further increase in Mach number. This decrease at higher Mach numbers is in sharp contrast to the secondary rise exhibited by the maximum lift curve of the NACA 66-series wing. Since this difference in maximum-lift characteristics is obviously of importance both structurally and aerodynamically, an analysis was made in reference 8 of pressure distributions for high Mach number and high angle-of-attack conditions in order to determine the reason for the difference.

This analysis showed that for the NACA 66-series wing the pressures over the forward part of the upper surface varied in a manner similar to those shown in figure 7. However, for the NACA 230-series wing the peak pressures moved downstream with increasing Mach number and caused a decrease in lift at the leading edge. As this change in the peak pressures was the only significant difference in the pressure distributions, it was conjectured that the main difference in maximum-lift characteristics at the higher Mach numbers is essentially a leading-edge effect and that airfoils having sharp leading edges, such as the NACA 66-series, exhibit the rise; whereas airfoils having blunt leading edges, such as the NACA 230 series, do not exhibit the rise.

The results of the present tests of the NACA 66-series wing with flaps indicate the same type of variation of maximum lift coefficient with Mach number as was obtained without flaps. Thus, it is further substantiated that the phenomenon is essentially a leading-edge effect as camber, camber location, and trailing-edge angle appear to have little or no effect on the type of variation of maximum normal-force coefficient with Mach number.

Typical section stalling characteristics.- An examination of the "carpet" plots of figure 5 shows that the types of stalling can be divided into three representative groups: low-speed stall ($M = 0.200$), moderate-speed stall ($M = 0.390$), and high-speed stall ($M = 0.535$). In order to give a clearer understanding of these three types of stalling, pressure distributions that show typical section stalling characteristics for the full-span flap configuration are presented in figures 9 to 11. As the typical section stalling characteristics are similar for all three configurations, a discussion of figures 9 to 11 also applies to the wing without flaps and to the wing with partial-span flaps.

The low-speed section stall is characterized by laminar separation of the flow from the leading edge (see reference 12) with an abrupt stall and a rapid flow breakdown. In figure 9 the pressure peaks can be observed to increase rapidly with increases in angle of attack until large adverse pressure gradients finally induce separation that causes a sharp flow breakdown at the leading edge. It can also be seen that little change in trailing-edge separation occurs before the stall.

The moderate-speed section stall was very different from that observed at low speed. Figure 10 shows that the moderate-speed section stall occurs slowly with increasing angle of attack and is due to trailing-edge separation gradually moving forward.

The high-speed section stall is also due to separation moving forward from the trailing edge. Figure 11 shows, however, that the high-speed section stall occurs more rapidly with increasing angle of attack than does the moderate-speed section stall.

Span-Load Distribution

A comparison between the low-speed experimental and calculated span-load distributions presented in figure 12 indicates fair agreement. The calculated span-load distributions which were determined by the method of reference 14 are based on five harmonics. For the wing with partial-span flaps better agreement can be obtained if the calculated span-load distributions are based on a greater number of harmonics. (See reference 15.) In figure 12(b), a comparison made at a normal-force coefficient of 0.90 for the wing without flaps shows good agreement between the low-speed experimental and calculated span-load distributions. A comparison between low-speed and high-speed experimental span-load distributions presented in figure 13 indicates that there is a slight inboard shift in the center of normal force at high speeds.

As can be seen in figure 14, the effect of Mach number on the inboard shift of the lateral center of normal force is very slight. A comparison of low-speed experimental and calculated lateral centers of normal force shows excellent agreement. For the wing with full-span flaps there is practically no variation of lateral center of normal force with normal-force coefficient. For the wing with partial-span flaps the lateral center of normal force shifts outboard with an increase in normal-force coefficient. The reason for this becomes apparent upon an examination of the span-load distributions presented in figures 12(a) and 13(a). It may also be noted that the lateral centers of normal force for the wing without flaps show good agreement with those obtained for the wing with full-span flaps.

Pitching-Moment Characteristics

The pitching-moment coefficients presented in figure 15 show that there is a much larger effect of Mach number at low angles of attack for the wing with flaps than for the wing without flaps. This effect is larger because the center of pressure is farther back on the chord and the effect of Mach number on the normal-force coefficient is larger for the wing with flaps as indicated in figure 6.

Figure 15 also shows that above an angle of attack of 5° for the wing without flaps the pitching-moment coefficient for a Mach number of 0.6 undergoes a large change because the center of pressure moves forward with the formation of local supersonic flow regions over the forward part of the wing. A similar change in pitching-moment coefficient associated with the same phenomenon can be seen for the wing with flaps at the highest Mach numbers.

For Mach numbers of 0.20 and 0.40 the pitching-moment coefficients for the wing without flaps show changes upon exceeding the low-drag range that are associated with the same phenomenon which causes normal-force-coefficient changes.

The stability at the stall encountered at various speeds for the three configurations is clearly shown in figure 15. For the wing with full-span flaps at the highest Mach number a more complete definition of the curve was prevented by structural limitations of the model support system.

Flap Normal-Force and Hinge-Moment Coefficients

A study of figure 16 indicates that the flap normal-force coefficient and flap hinge-moment coefficient show no large changes in the range of Mach numbers and wing normal-force coefficients covered. In general, the shapes of the flap normal-force and hinge-moment curves are very similar for a given configuration and Mach number. This similarity results from the fact that the position of the center of pressure on the flap is almost the same for all conditions, and thus the hinge moment is nearly a direct function of the normal force.

Figure 16 also shows that there is an increase in both flap normal-force coefficient and hinge-moment coefficient with Mach number. This increase with Mach number is less than 20 percent through the range tested. The maximum variation of either flap normal-force or hinge-moment coefficient with wing normal-force coefficient is smaller, and is less than 10 percent in most cases.

CONCLUSIONS

Results of a high-speed wind-tunnel investigation of a tapered wing of NACA 66-series airfoil sections with both partial- and full-span split flaps deflected 60° indicated:

1. The maximum normal-force curves for the wing with flaps were somewhat similar in shape to the maximum lift curve for the wing without flaps, although Mach number effects became apparent at lower speeds and were larger for the wing with flaps.

2. For the wing with partial-span split flaps the maximum normal-force coefficient increased from a value of 1.69 at a Mach number of 0.145 to a low-speed peak value of 1.73 at a Mach number of 0.200; then decreased to a value of 1.53 at a Mach number of 0.295; and then remained constant to a Mach number of 0.485 after which it increased rapidly to a value of 1.79 at a Mach number of 0.585 (limit of maximum normal-force tests).

3. For the wing with full-span split flaps the maximum normal-force coefficient increased from a value of 1.92 at a Mach number of 0.145 to a low-speed peak value of 2.09 at a Mach number of 0.200; then decreased rapidly to a value of 1.87 at a Mach number of 0.300; and then increased slowly to a value of 1.92 at a Mach number of 0.485 after which it rose rapidly to a value of 2.22 at a Mach number of 0.550 (limit of maximum normal-force tests).

4. There is further evidence that the rapid rise in maximum lift coefficient at higher Mach numbers is due to the sharp leading edge of the wing as camber, camber location, and trailing-edge angle appeared to have little or no effect on the rise.

5. Mach number had only a slight effect on the shift of lateral center of normal force for angles of attack below the stall.

6. For the Mach number range of the tests the maximum variation of either flap normal-force or hinge-moment coefficient with Mach number and wing normal-force coefficient were less than 20 percent and 10 percent, respectively.

Langley Aeronautical Laboratory
National Advisory Committee for Aeronautics
Langley Field, Va., September 11, 1948

REFERENCES

1. Muse, Thomas C.: Some Effects of Reynolds and Mach Numbers on the Lift of an NACA 0012 Rectangular Wing in the NACA 19-Foot Pressure Tunnel. NACA CB No. 3E29, 1943.

2. Cleary, Harold E.: Effects of Compressibility on Maximum Lift Coefficients for Six Propeller Airfoils. NACA ACR No. L4L21a, 1945.

3. Nissen, James M., and Gadeberg, Burnett L.: Effect of Mach and Reynolds Numbers on the Power-Off Maximum Lift Coefficient Obtainable on a P-39N-1 Airplane as Determined in Flight. NACA ACR No. 4F28, 1944.

4. Rhode, Richard V.: Correlation of Flight Data on Limit Pressure Coefficients and Their Relation to High-Speed Burbling and Critical Tail Loads. NACA ACR No. L4I27, 1944.

5. Pearson, E. O., Jr., Evans, A. J., and West, F. E., Jr.: Effects of Compressibility on the Maximum Lift Characteristics and Spanwise Load Distribution of a 12-Foot-Span Fighter-Type Wing of NACA 230-Series Airfoil Sections. NACA ACR No. L5G10, 1945.

6. Pearson, E. O., Jr.: Effect of Compressibility on the Distribution of Pressures over a Tapered Wing of NACA 230-Series Airfoil Sections. NACA TN No. 1390, 1947.

7. Furlong, G. Chester, and Fitzpatrick, James E.: Effects of Mach Number and Reynolds Number on the Maximum Lift Coefficient of a Wing of NACA 230-Series Airfoil Sections. NACA TN No. 1299, 1947.

8. Cooper, Morton, and Korycinski, Peter F.: The Effects of Compressibility on the Lift, Pressure, and Load Characteristics of a Tapered Wing of NACA 66-Series Airfoil Sections. NACA TN No. 1697, 1948.

9. Wall, Nancy E.: Chordwise Pressure Distributions on a 12-Foot-Span Wing of NACA 66-Series Airfoil Sections up to a Mach Number of 0.60. NACA TN No. 1696, 1948.

10. Von Doenhoff, Albert E., and Tetervin, Neal: Investigation of the Variation of Lift Coefficient with Reynolds Number at a Moderate Angle of Attack on a Low-Drag Airfoil. NACA CB, Nov. 1942.

11. Göthert, B.: Plane and Three-Dimensional Flow at High Subsonic Speeds. NACA TM No. 1105, 1946.

12. Jacobs, Eastman N., and Sherman, Albert: Airfoil Section Characteristics as Affected by Variations of the Reynolds Number. NACA Rep. No. 586, 1937.

13. Stack, John, Fedziuk, Henry A., and Cleary, Harold E.: Preliminary Investigation of the Effect of Compressibility on the Maximum Lift Coefficient. NACA ACR, Feb. 1943.

14. Anon.: Spanwise Air-Load Distribution. ANC-1(1), Army-Navy-Commerce Committee on Aircraft Requirements. U.S. Govt. Printing Office, April 1938.

15. Pearson, H. A.: Span Load Distribution for Tapered Wings with Partial-Span Flaps. NACA Rep. No. 585, 1937.

TABLE I

AIRFOIL ORDINATES OF NACA 66-SERIES WING

[Stations and ordinates are given in percent of airfoil chord]

Root section				Tip section			
Upper surface		Lower surface		Upper surface		Lower surface	
Station	Ordinate	Station	Ordinate	Station	Ordinate	Station	Ordinate
0	0	0	0	0	0	0	0
.43	1.21	.57	−1.15	.37	1.24	.63	−1.11
.68	1.46	.82	−1.37	.61	1.50	.89	−1.32
1.17	1.82	1.33	−1.68	1.09	1.89	1.41	−1.61
2.41	2.50	2.59	−2.25	2.32	2.61	2.68	−2.13
4.90	3.50	5.10	−3.08	4.79	3.70	5.21	−2.87
7.39	4.28	7.61	−3.73	7.28	4.56	7.72	−3.44
9.89	4.97	10.11	−4.28	9.78	5.31	10.22	−3.93
14.89	6.05	15.11	−5.15	14.79	6.50	15.21	−4.70
19.90	6.89	20.10	−5.83	19.81	7.43	20.19	−5.29
24.92	7.55	25.08	−6.34	24.83	8.16	25.17	−5.74
29.93	8.05	30.07	−6.74	29.86	8.71	30.14	−6.08
34.95	8.41	35.05	−7.02	34.90	9.11	35.10	−6.32
39.97	8.63	40.03	−7.18	39.94	9.36	40.06	−6.46
44.99	8.73	45.01	−7.26	44.98	9.47	45.03	−6.52
50.01	8.69	49.99	−7.22	50.03	9.43	49.98	−6.48
55.04	8.50	54.96	−7.06	55.08	9.23	54.93	−6.34
60.07	8.11	59.93	−6.74	60.14	8.80	59.86	−6.05
65.10	7.46	64.90	−6.20	65.19	8.08	64.81	−5.58
70.10	6.52	69.90	−5.42	70.20	7.07	69.80	−4.86
75.09	5.43	74.91	−4.50	75.18	5.89	74.82	−4.03
80.08	4.23	79.93	−3.49	80.15	4.59	79.85	−3.11
85.05	2.99	84.95	−2.44	85.11	3.26	84.89	−2.17
90.03	1.76	89.97	−1.41	90.06	1.94	89.94	−1.24
95.01	.68	94.99	−.52	95.02	.76	94.98	−.43
100	0	100	0	100	0	100	0
Leading-edge radius = 1.475c Slope of radius through leading edge = 0.058				Leading-edge radius = 1.475c Slope of radius through leading edge = 0.117			

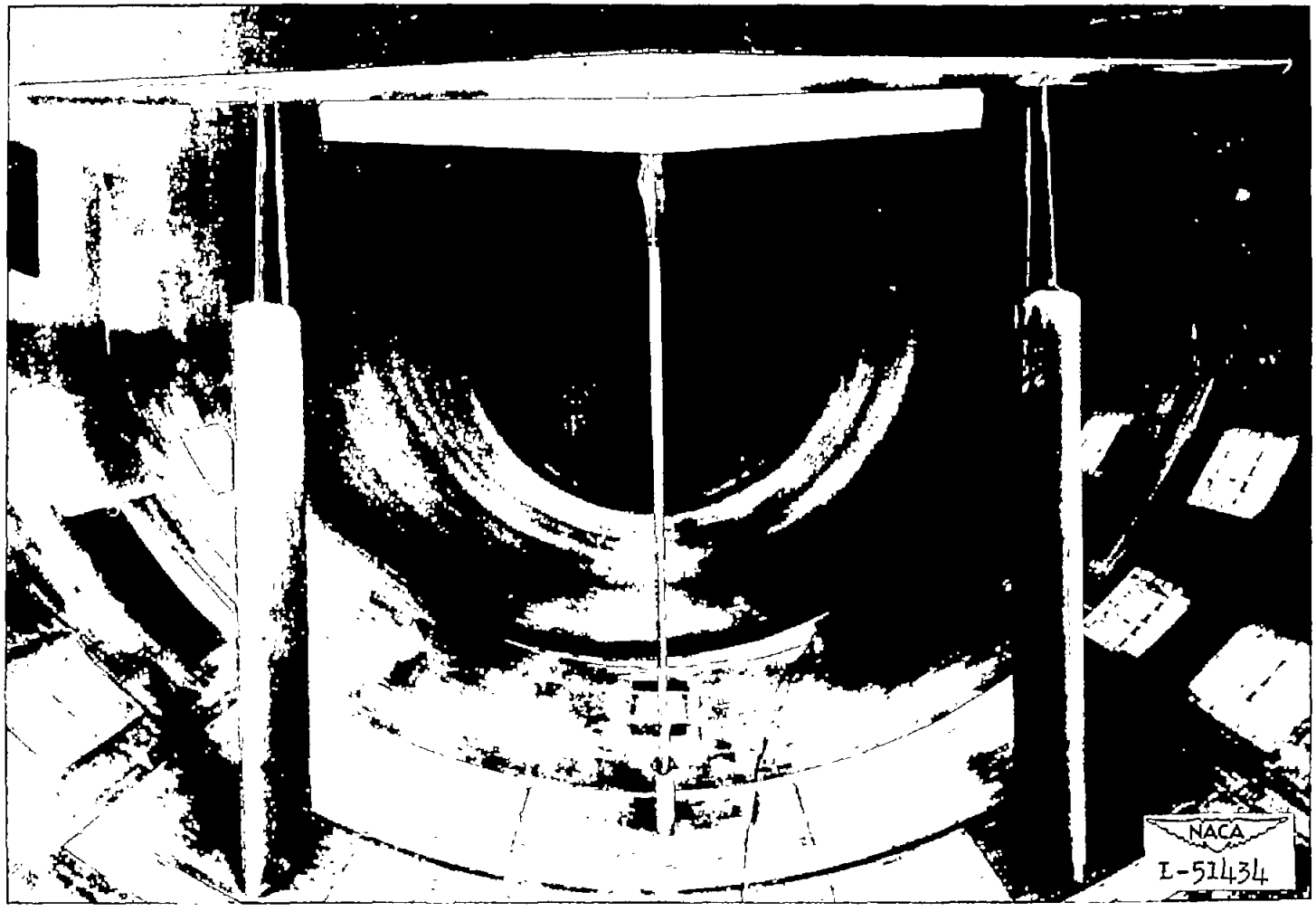

(a) Wing with partial-span flaps.

Figure 1.- Front view of test wing installed in Langley 16-foot high-speed tunnel.

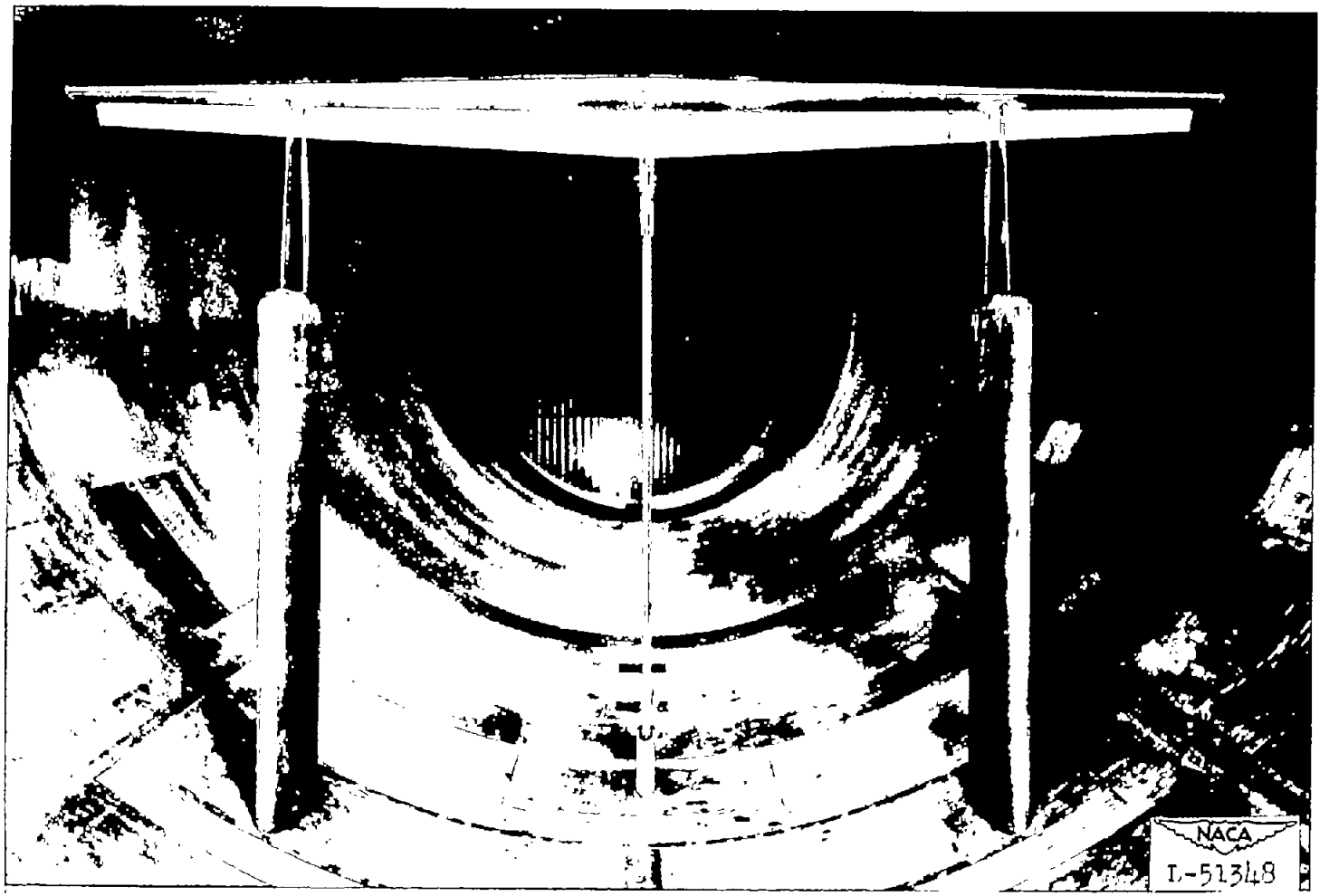

(b) Wing with full-span flaps.

Figure 1.- Concluded.

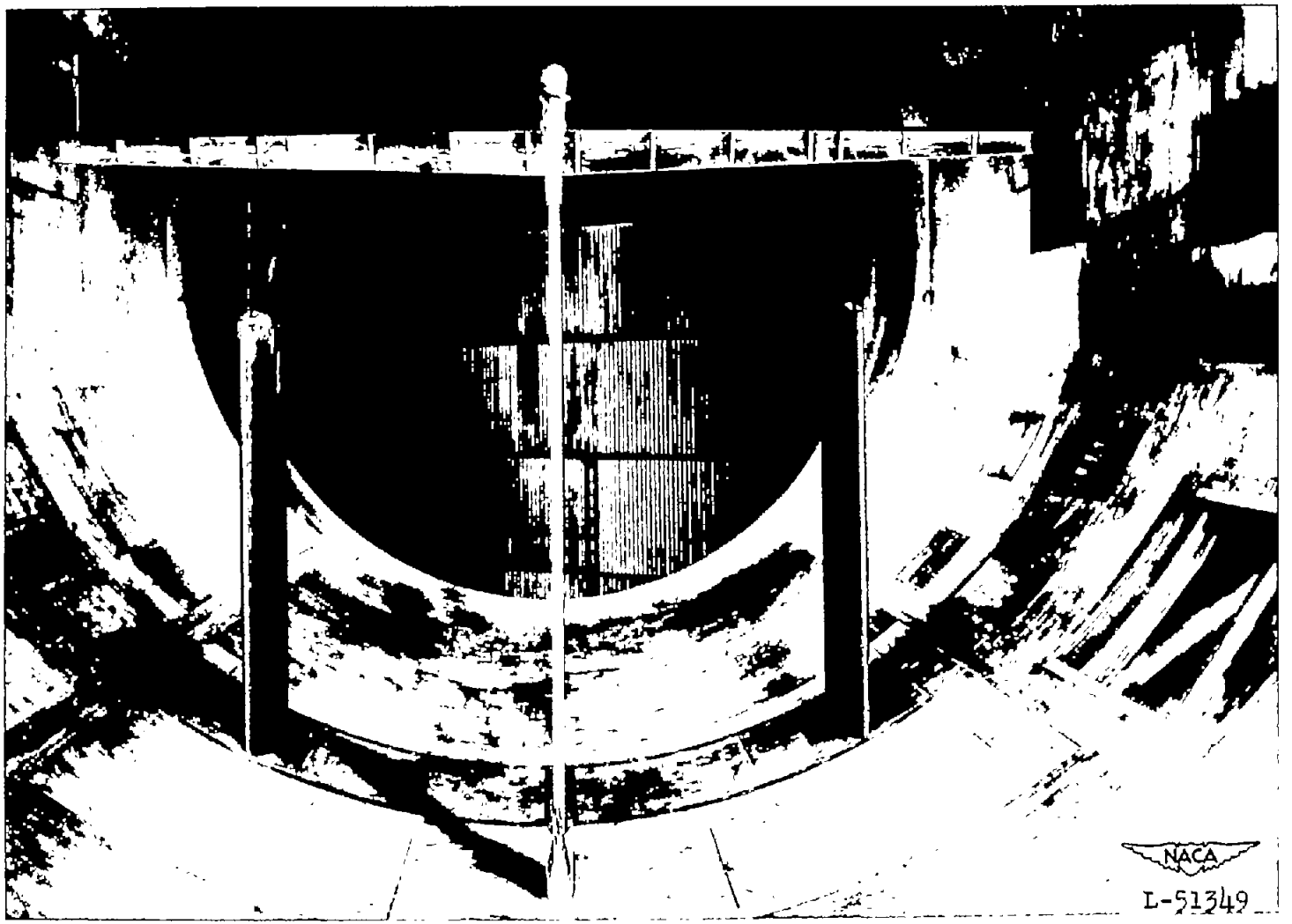

Figure 2.- Rear view of test wing with full-span flaps.

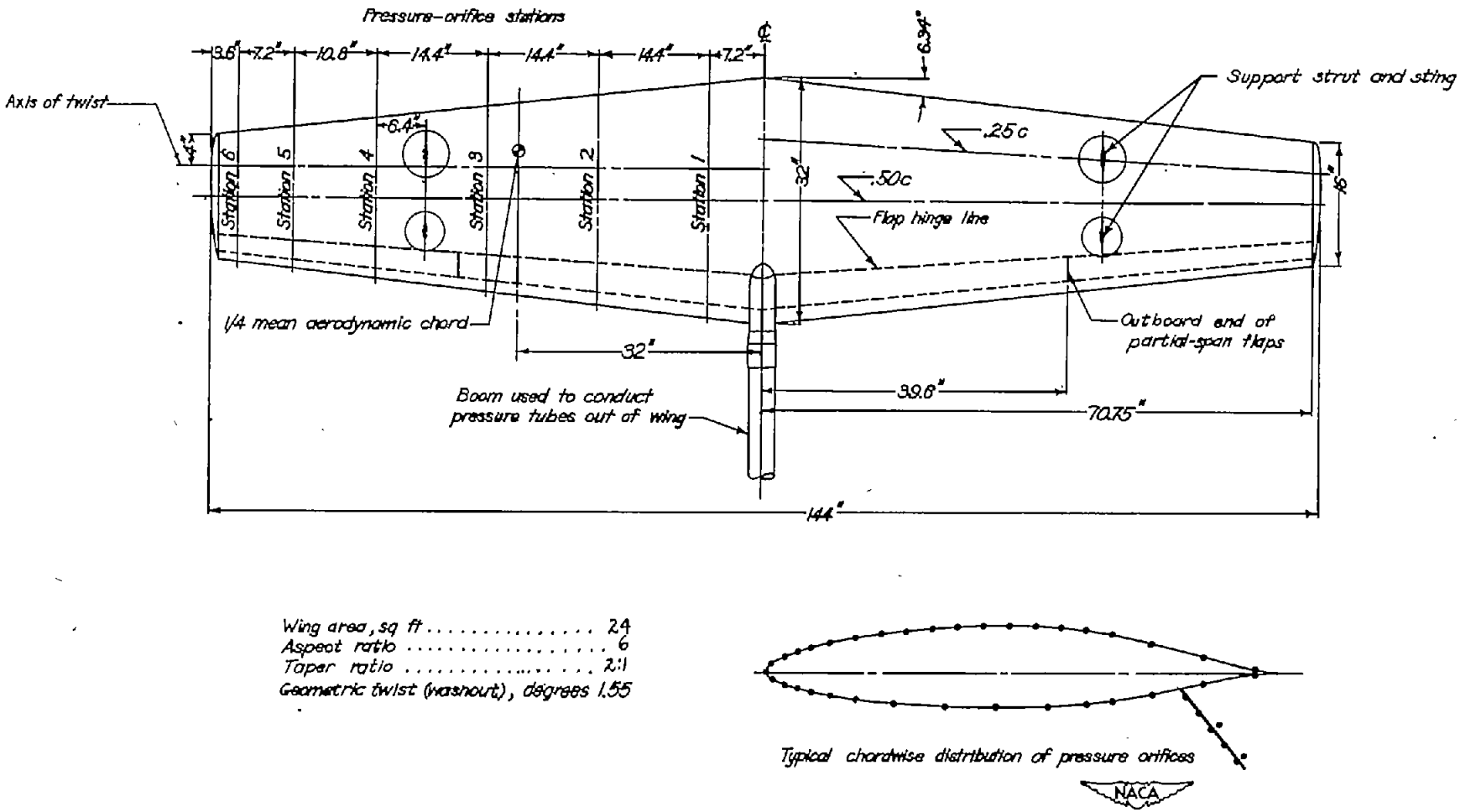

Figure 3.—Principal wing dimensions and locations of pressure orifices.

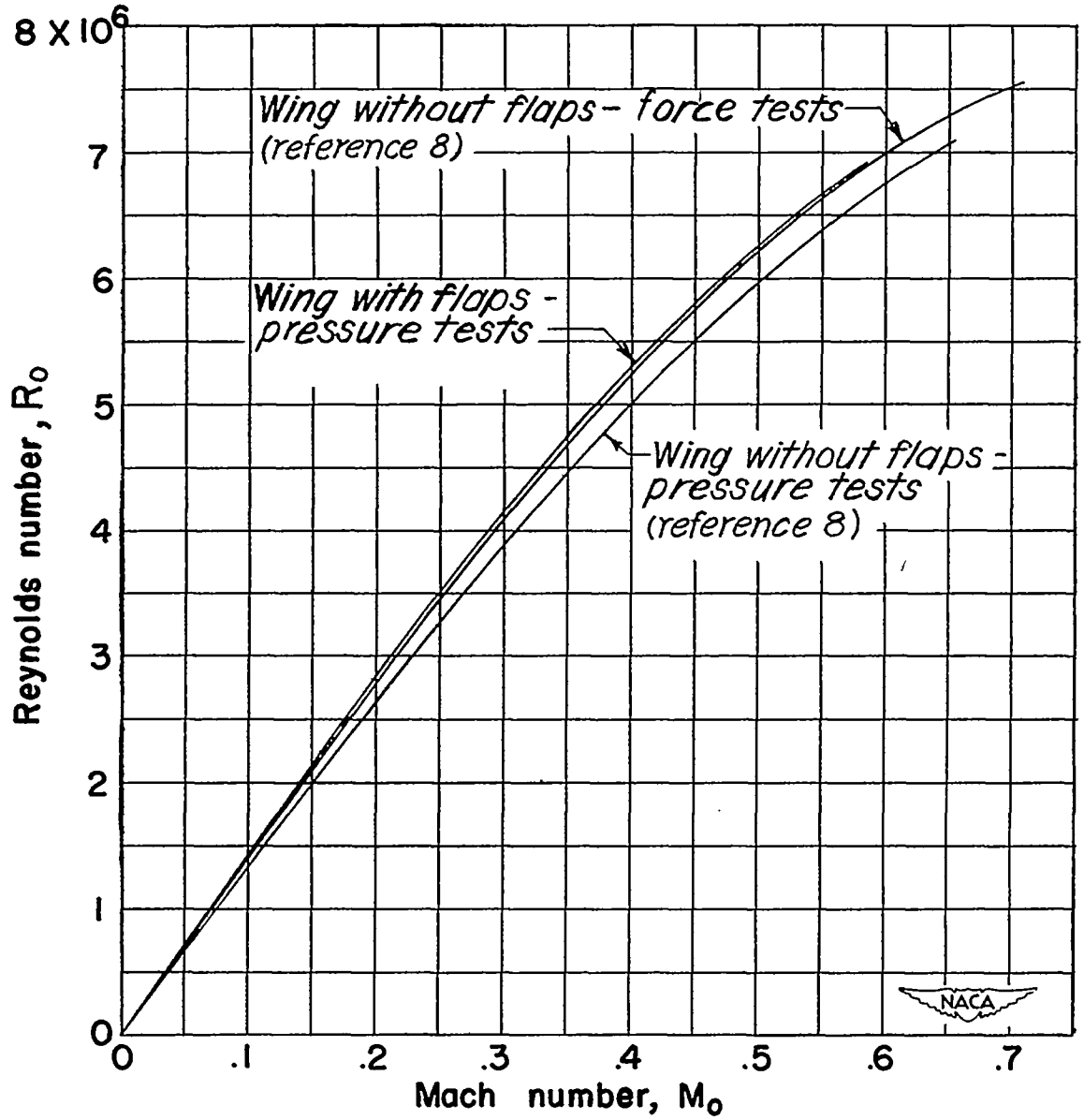

Figure 4.— Variation of average test Reynolds number with Mach number.

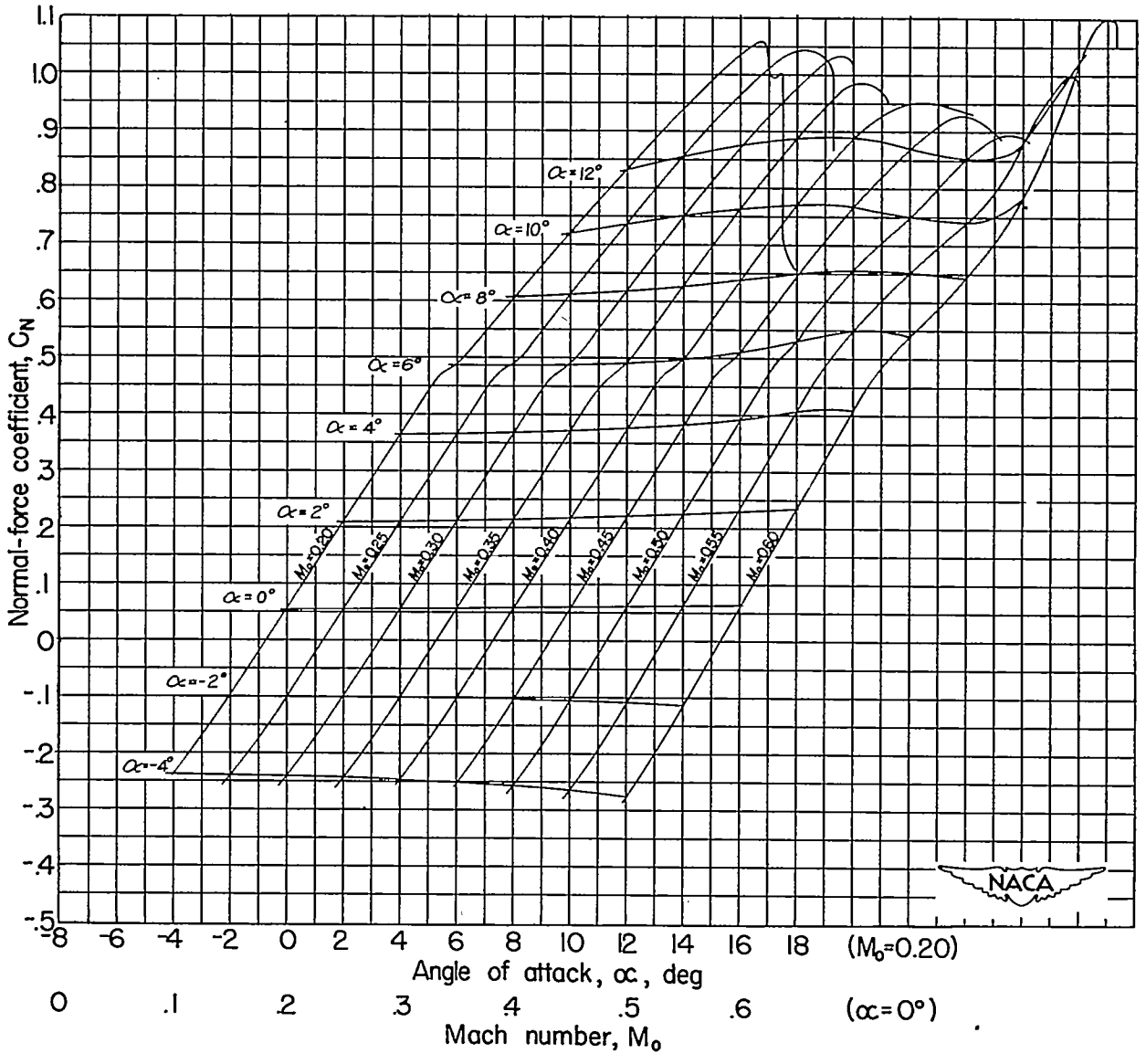

(a) Wing without flaps (reference 8).

Figure 5.—Wing normal-force coefficient as a function of angle of attack and Mach number.

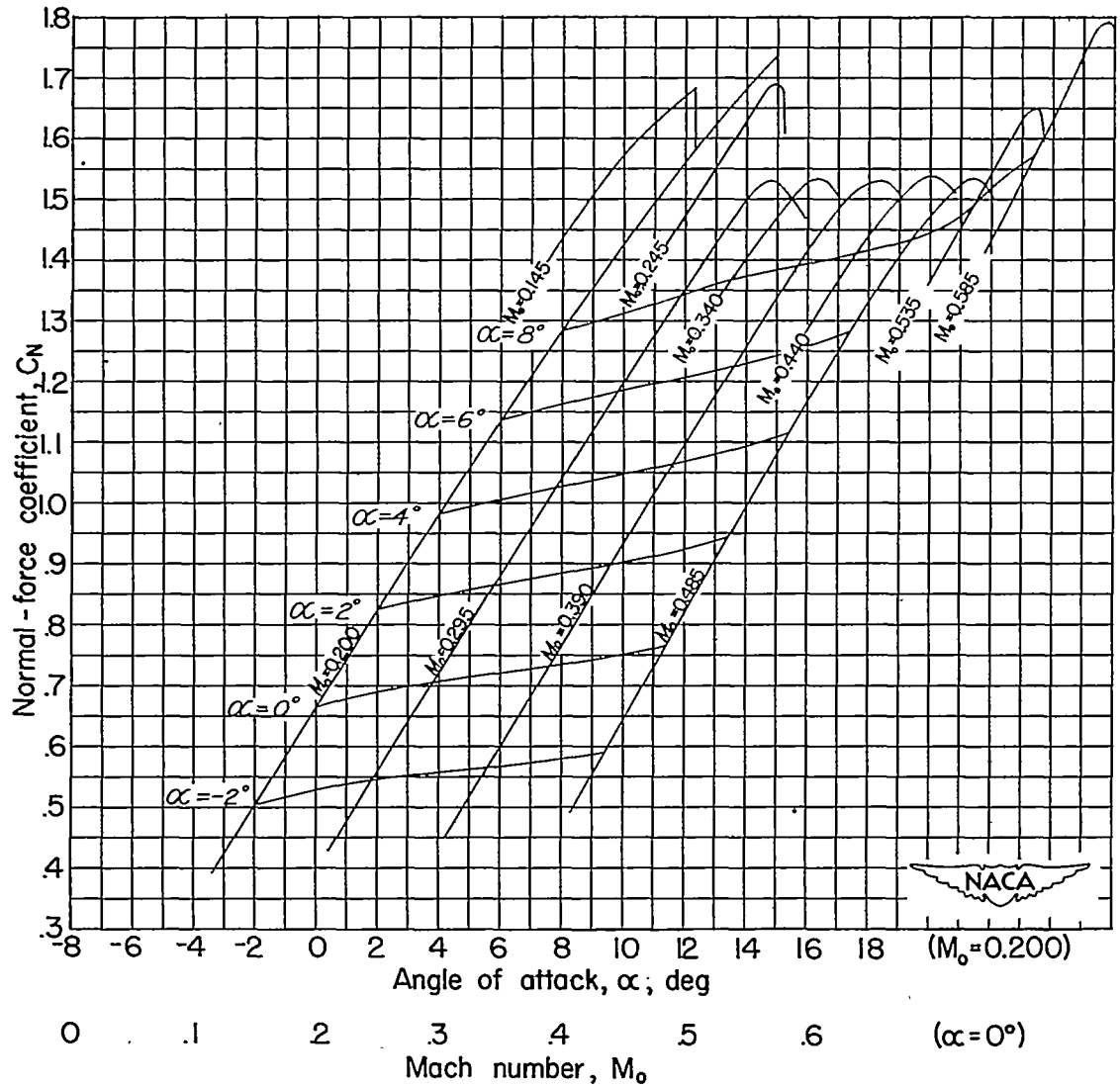

(b) Wing with partial-span flaps.

Figure 5.—Continued.

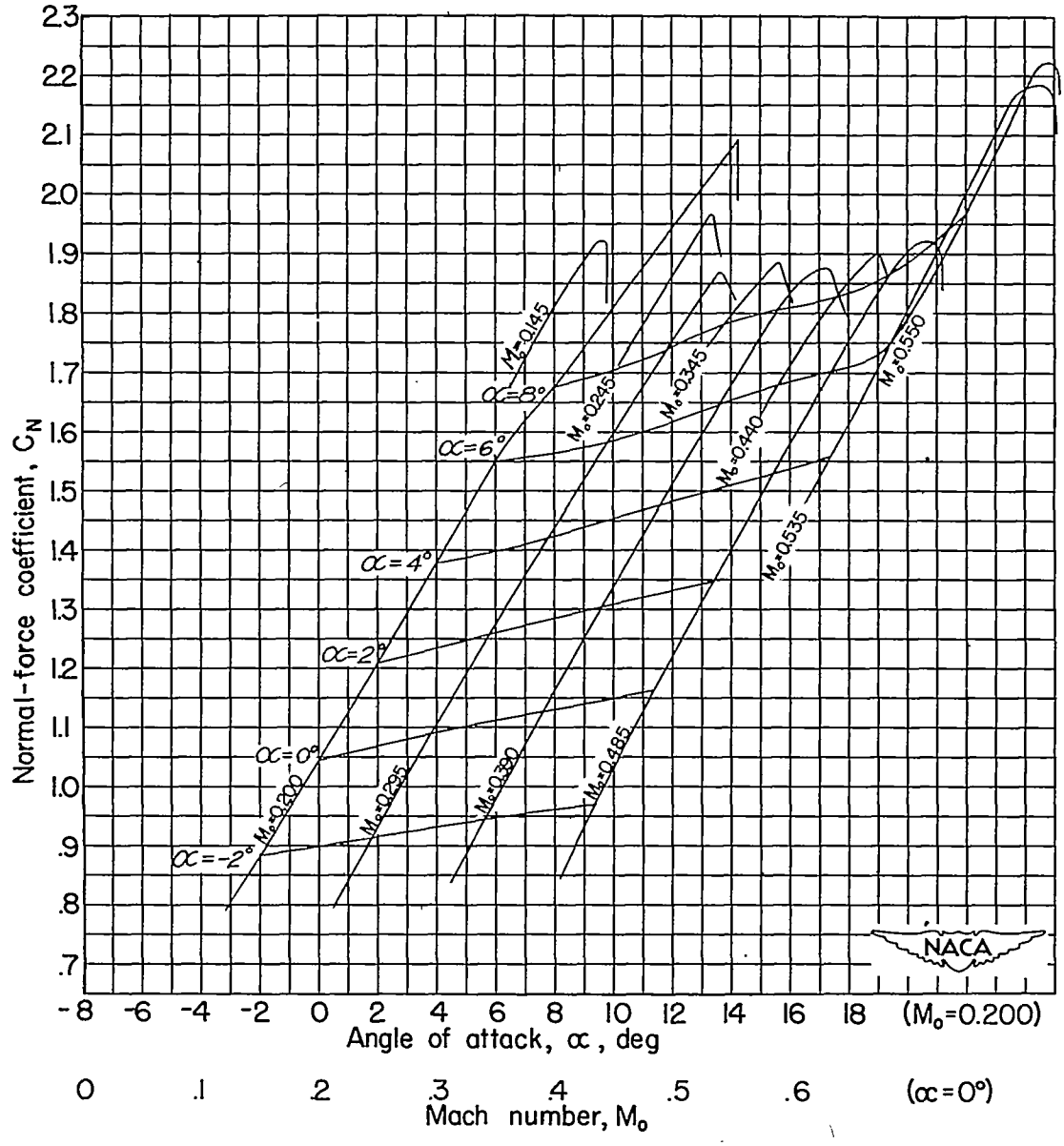

(c) Wing with full-span flaps.

Figure 5.—Concluded.

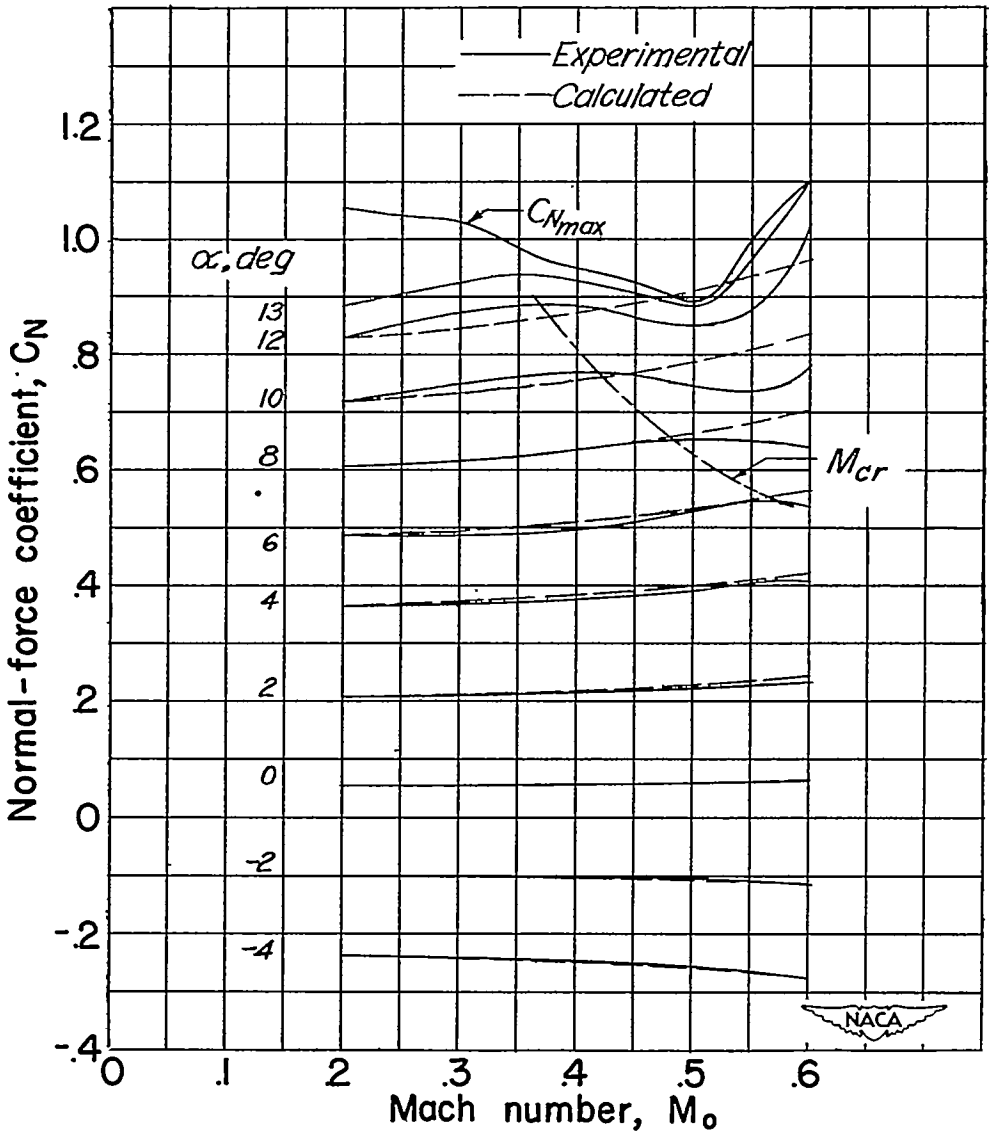

(a) Wing without flaps (reference 8).

Figure 6.- Comparison of experimental and calculated variation of normal-force coefficient with Mach number for several angles of attack.

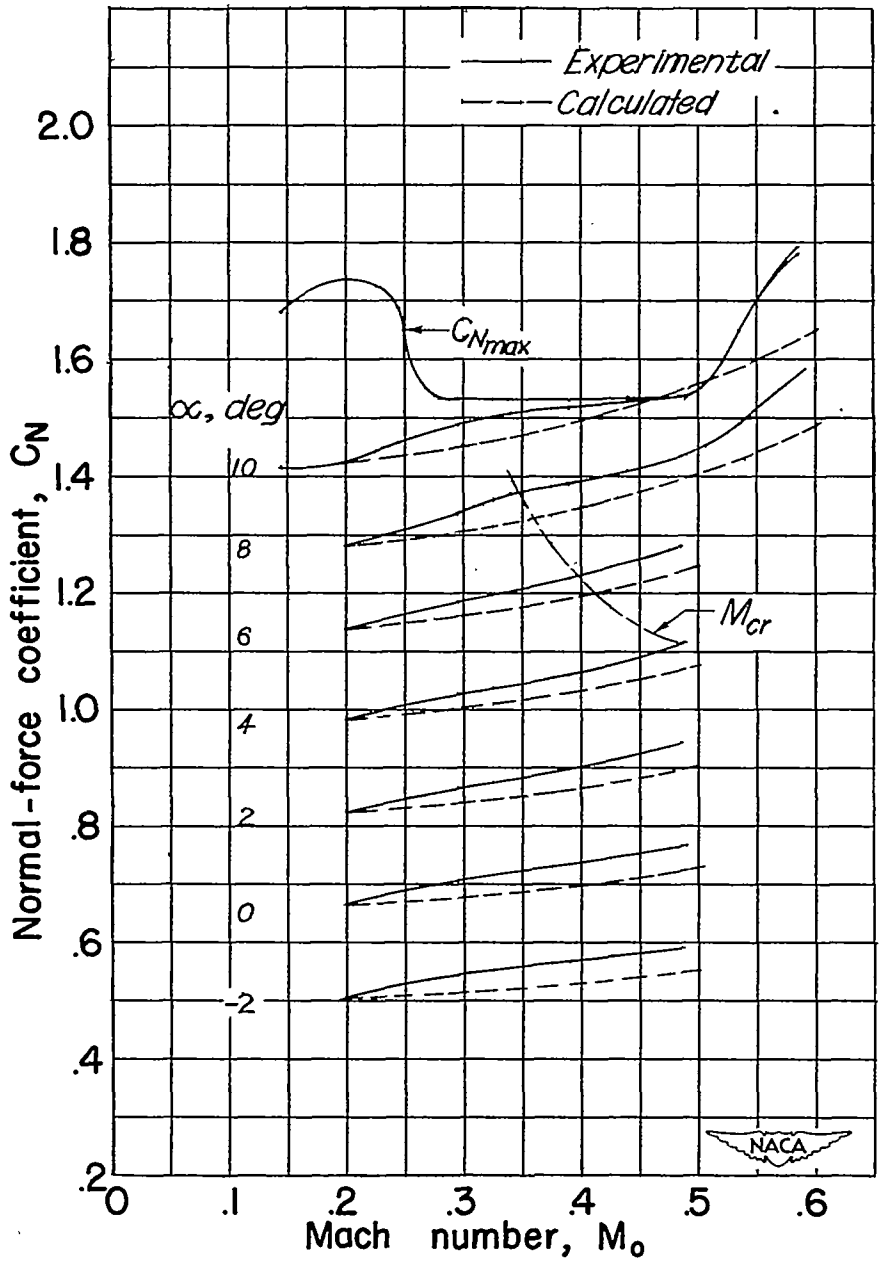

(b)Wing with partial-span flaps.

Figure 6.– Continued .

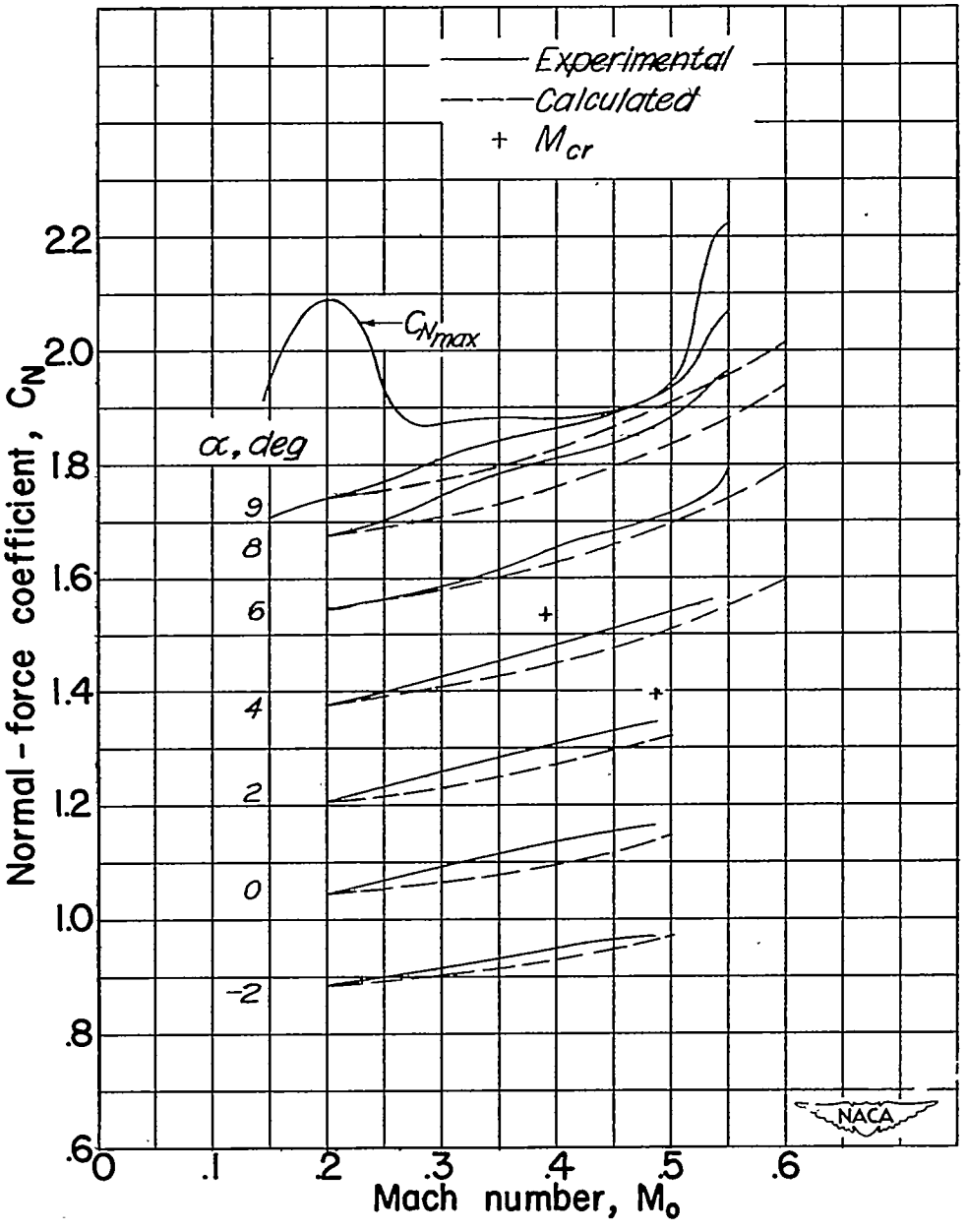

(c) Wing with full-span flaps.

Figure 6.- Concluded.

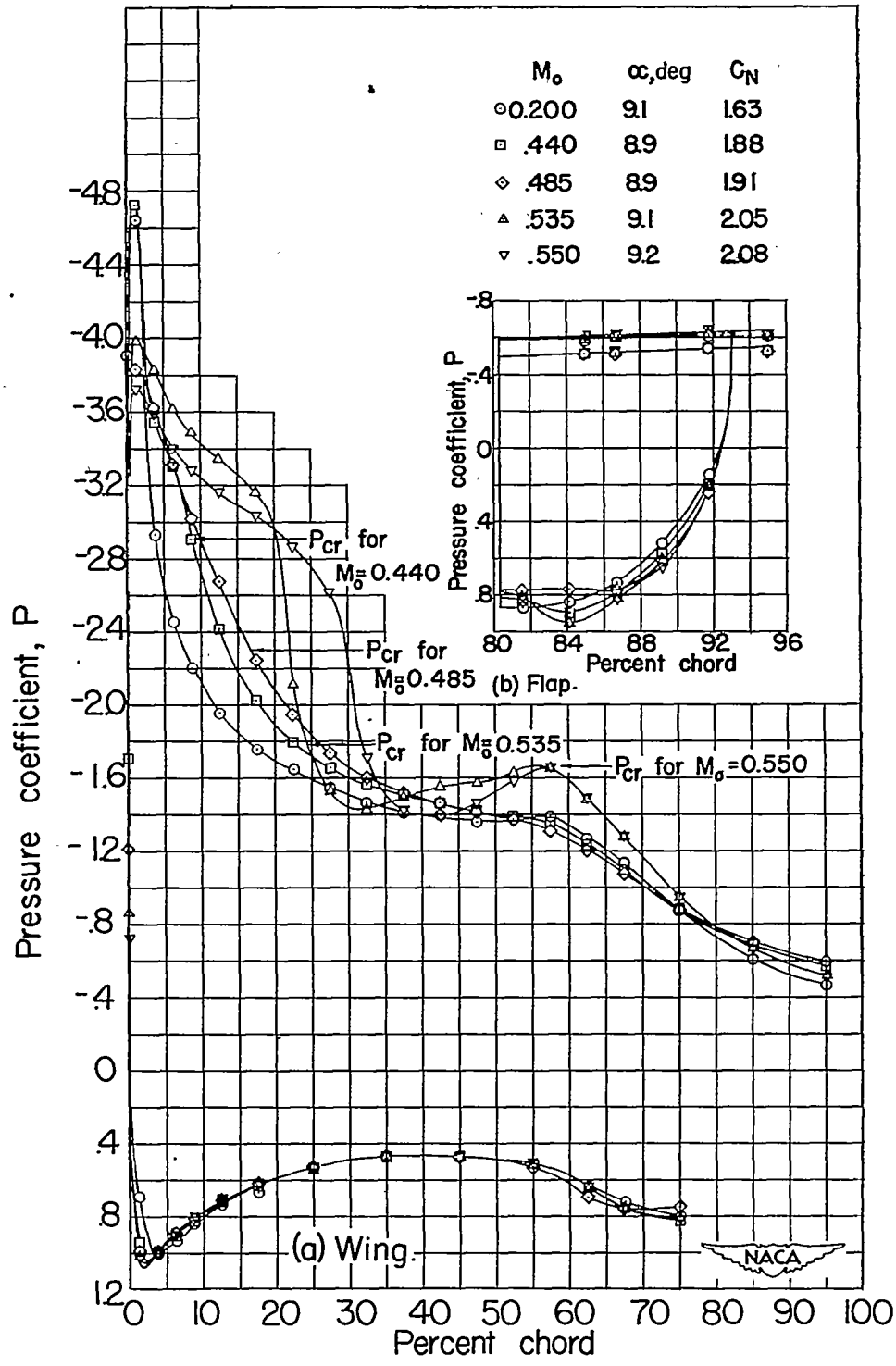

Figure 7.— Effect of Mach number on pressure distribution at station 3 of the wing with full-span flaps for an angle of attack of approximately 9°.

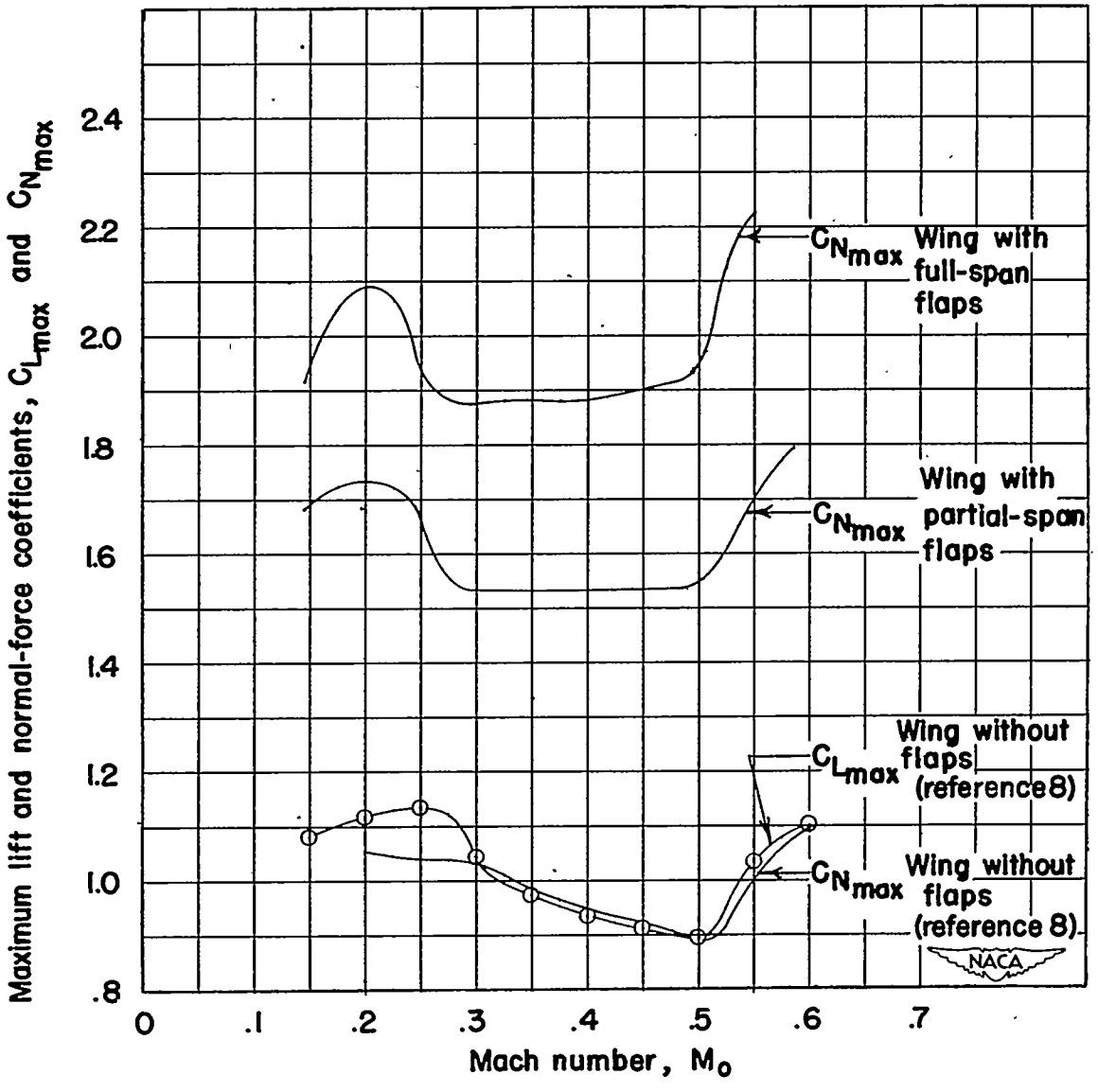

Figure 8 .——Variation of maximum lift and normal-force coefficients with Mach number.

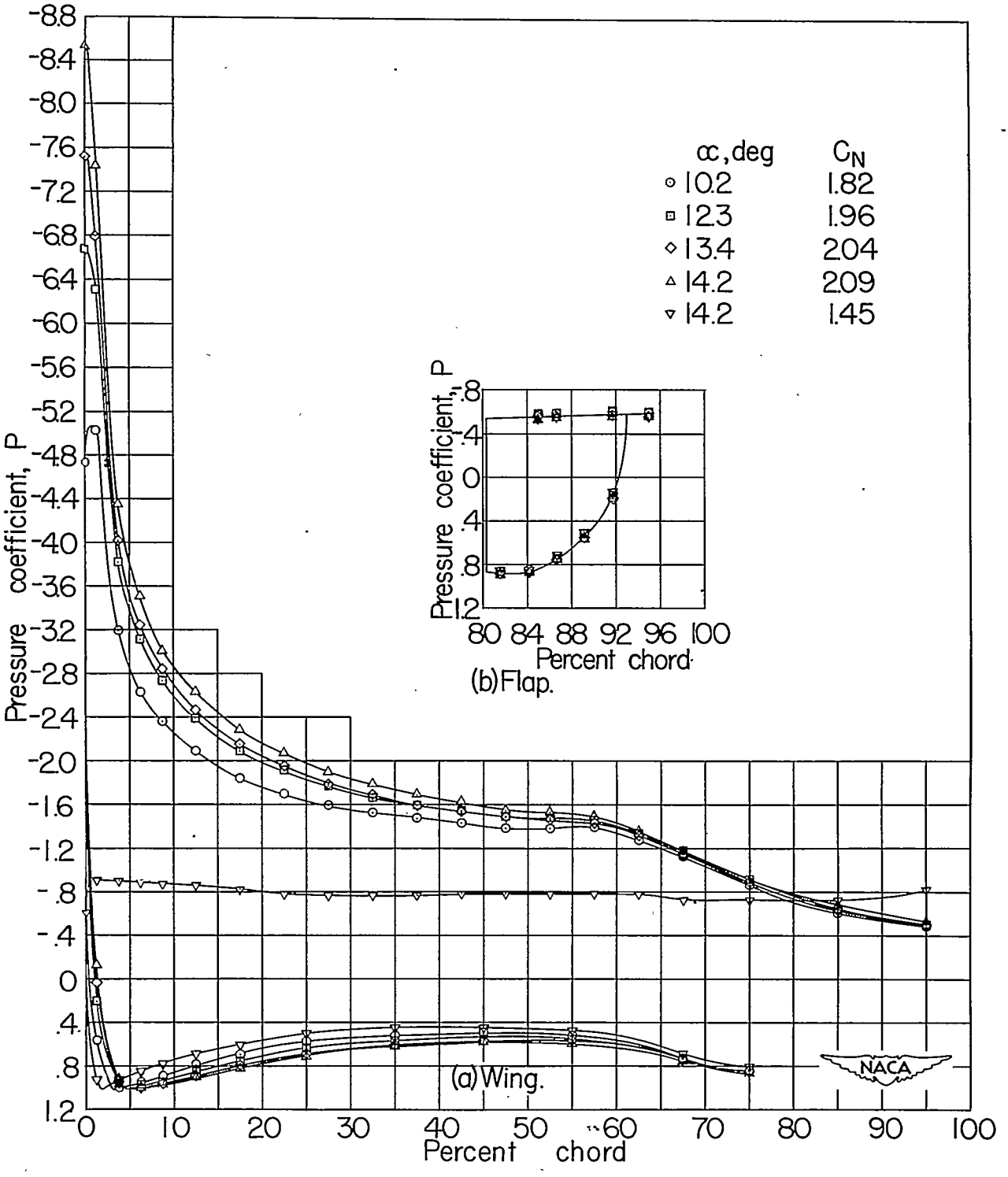

Figure 9.- Variation of pressure distributions at station 3 with angle of attack for wing with full-span flaps at a Mach number of 0.200.

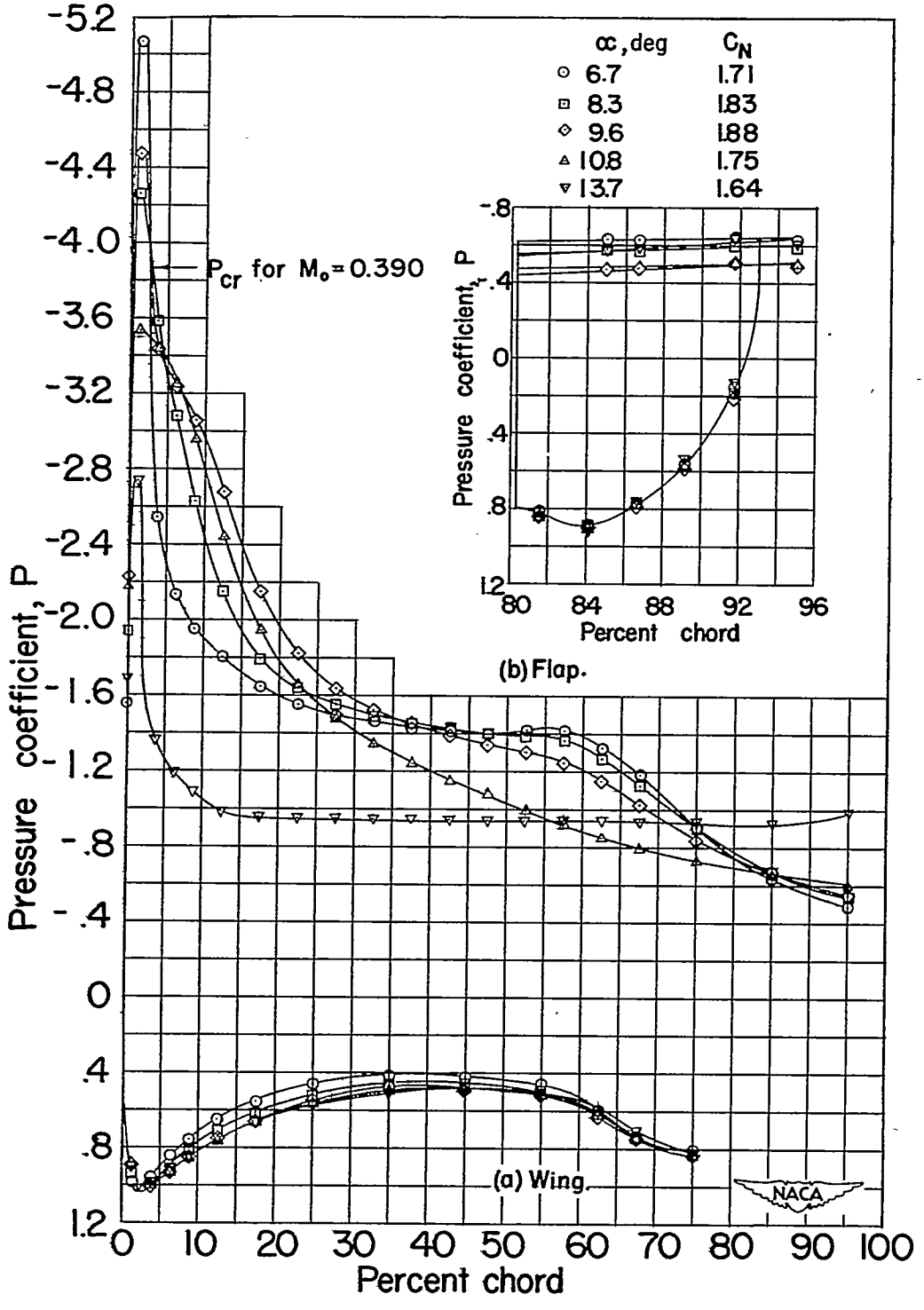

Figure 10.— Variation of pressure distributions at station 3 with angle of attack for the wing with full-span flaps at a Mach number of 0.390 .

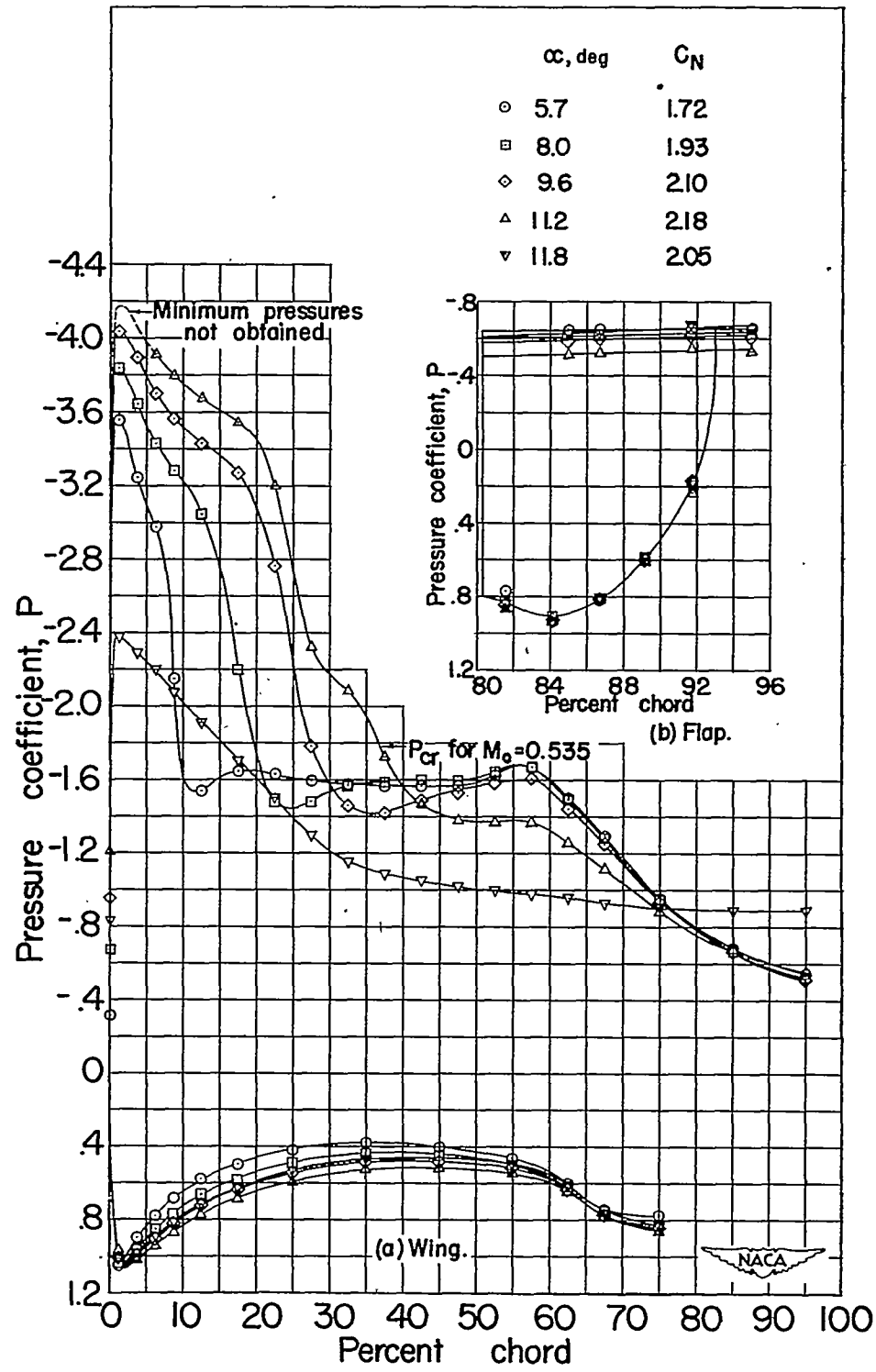

Figure 11.— Variation of pressure distributions at station 3 with angle of attack for wing with full-span flaps at a Mach number of 0.535.

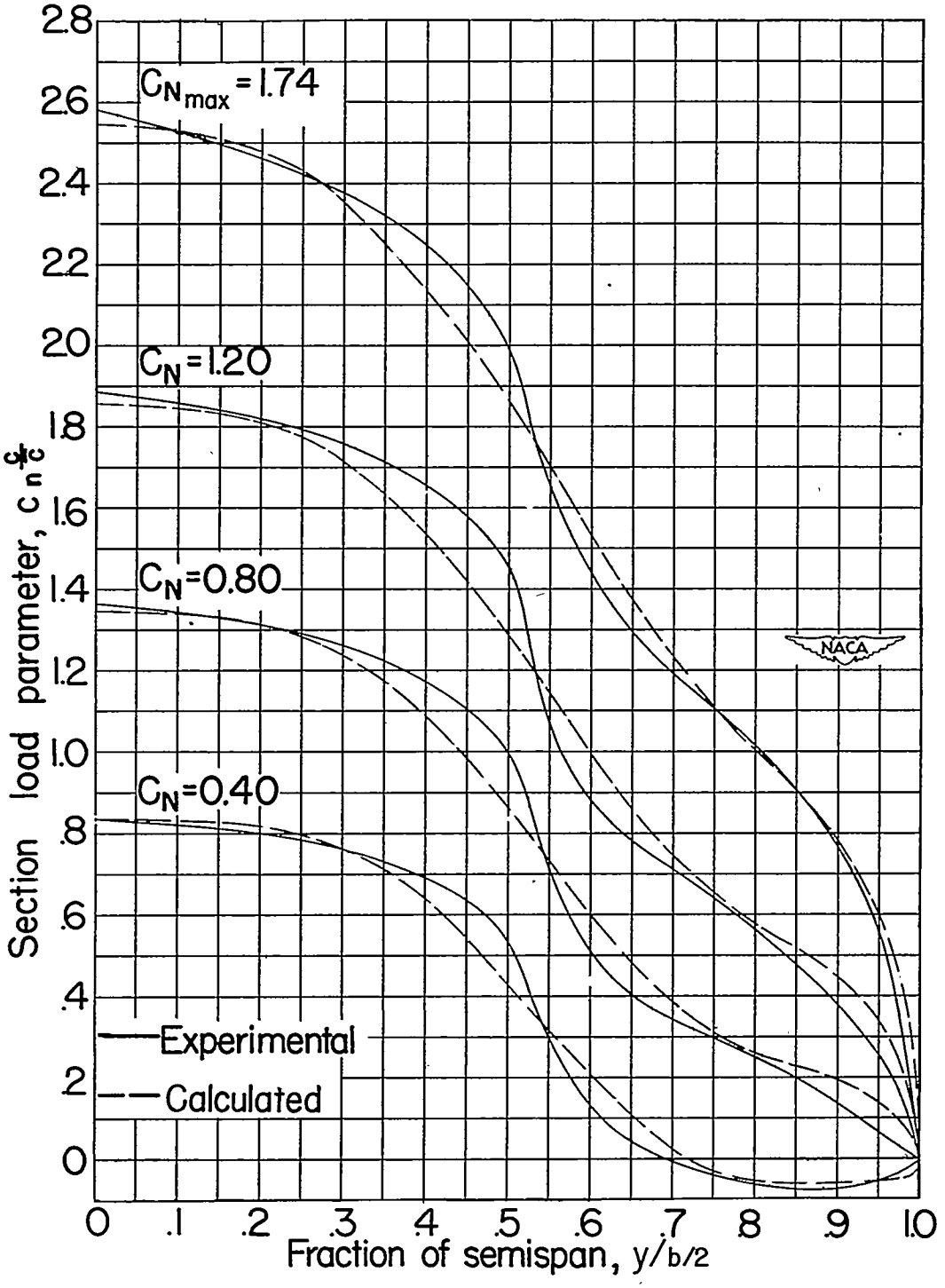

(a) Wing with partial-span flaps.

Figure 12. – Comparison of experimental and calculated span load distribution for representative normal-force coefficients at a Mach number of 0.200.

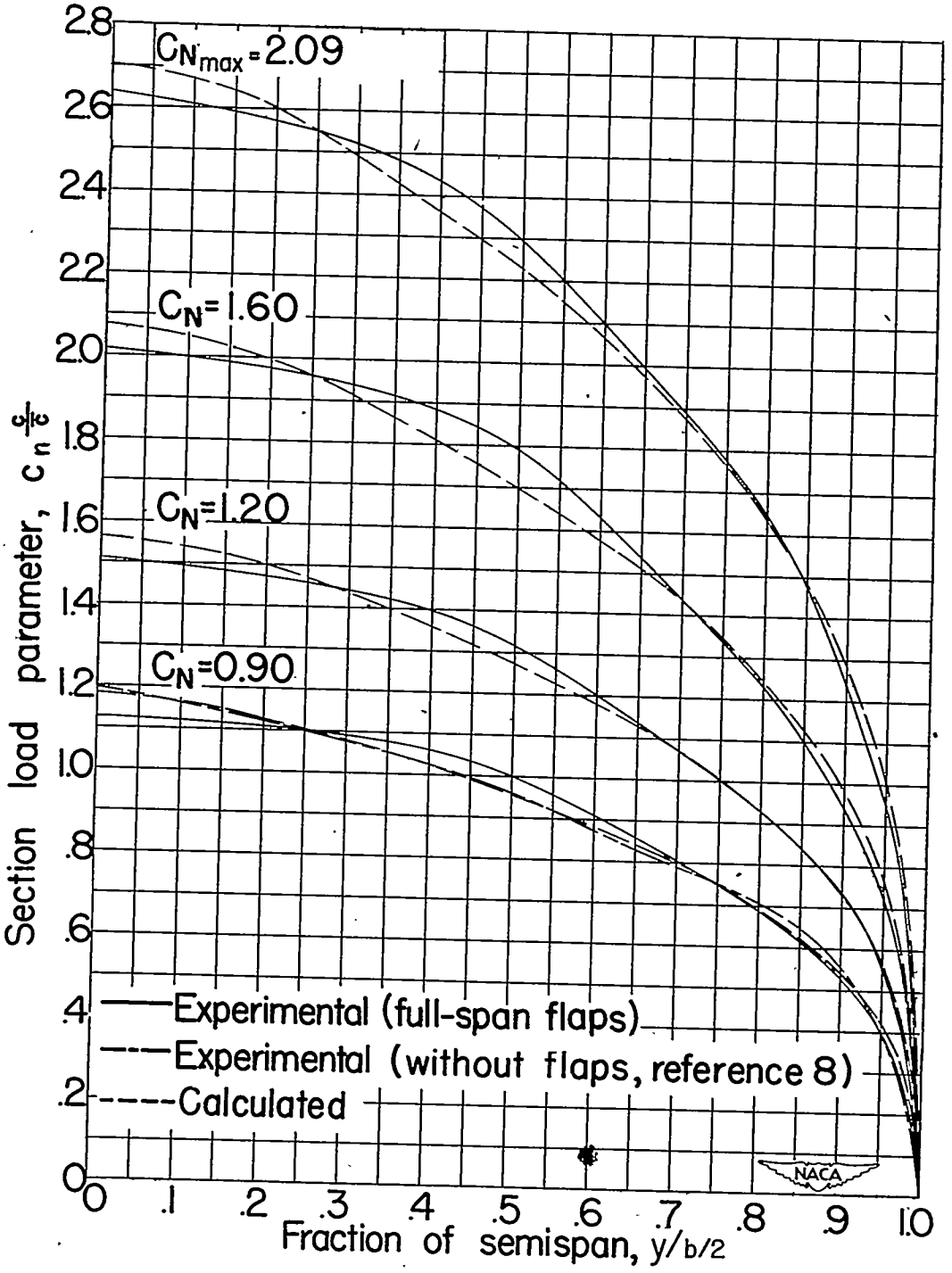

(b) Wing with full-span flaps.

Figure 12.- Concluded.

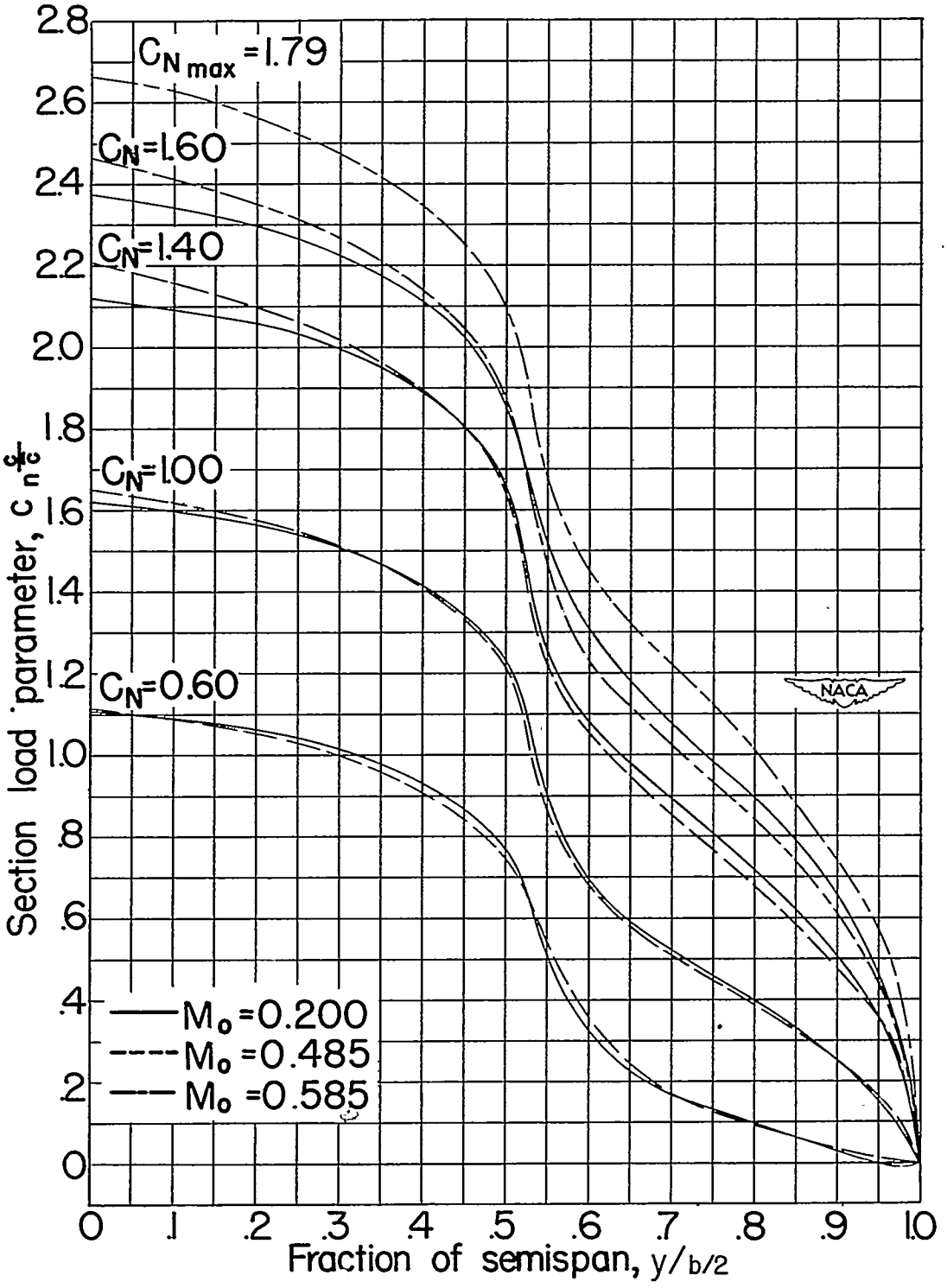

(a) Wing with partial-span flaps.

Figure 13.- Effect of Mach number on span load distributions for representative normal-force coefficients.

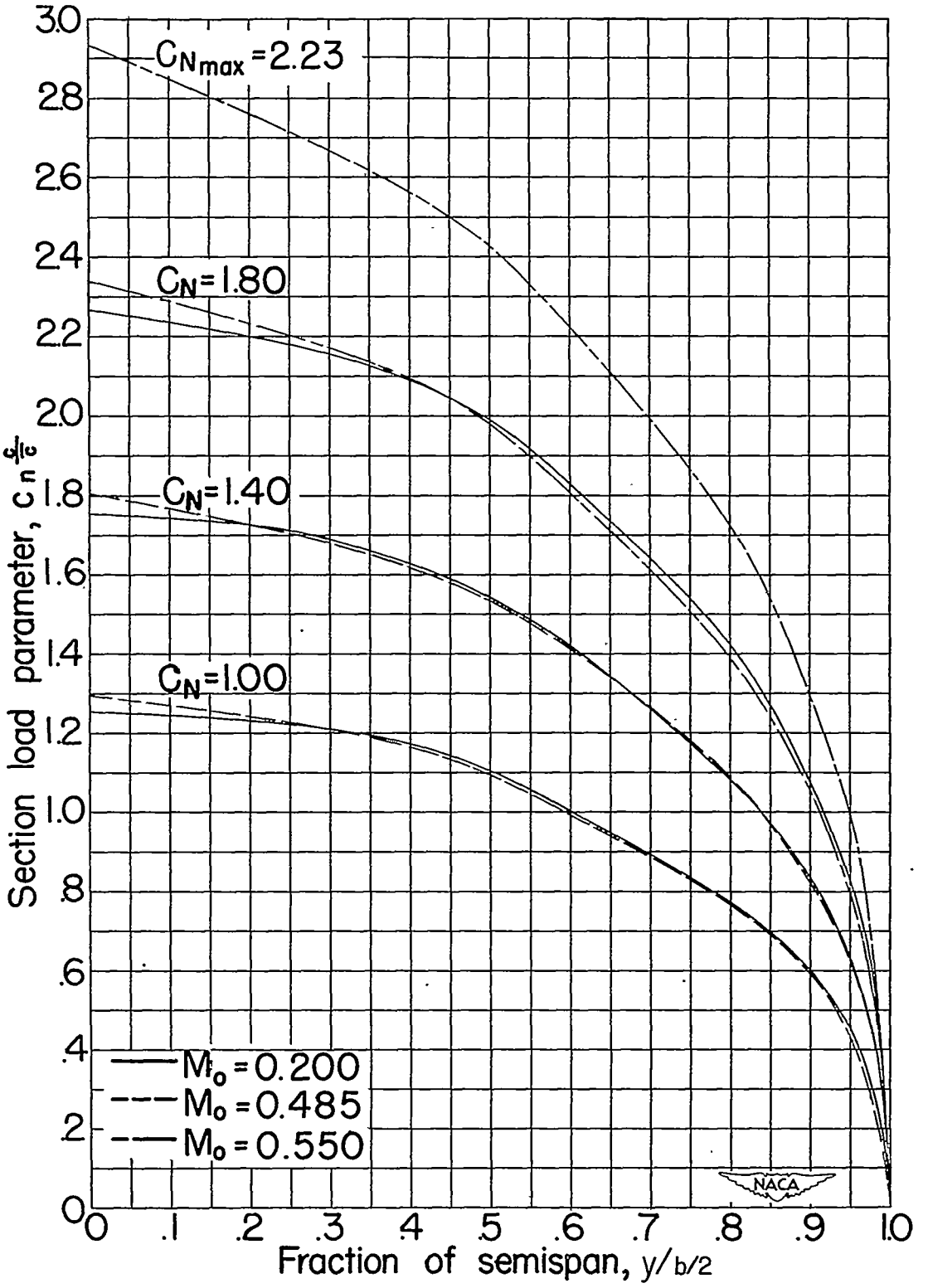

(b) Wing with full-span flaps.

Figure 13.- Concluded.

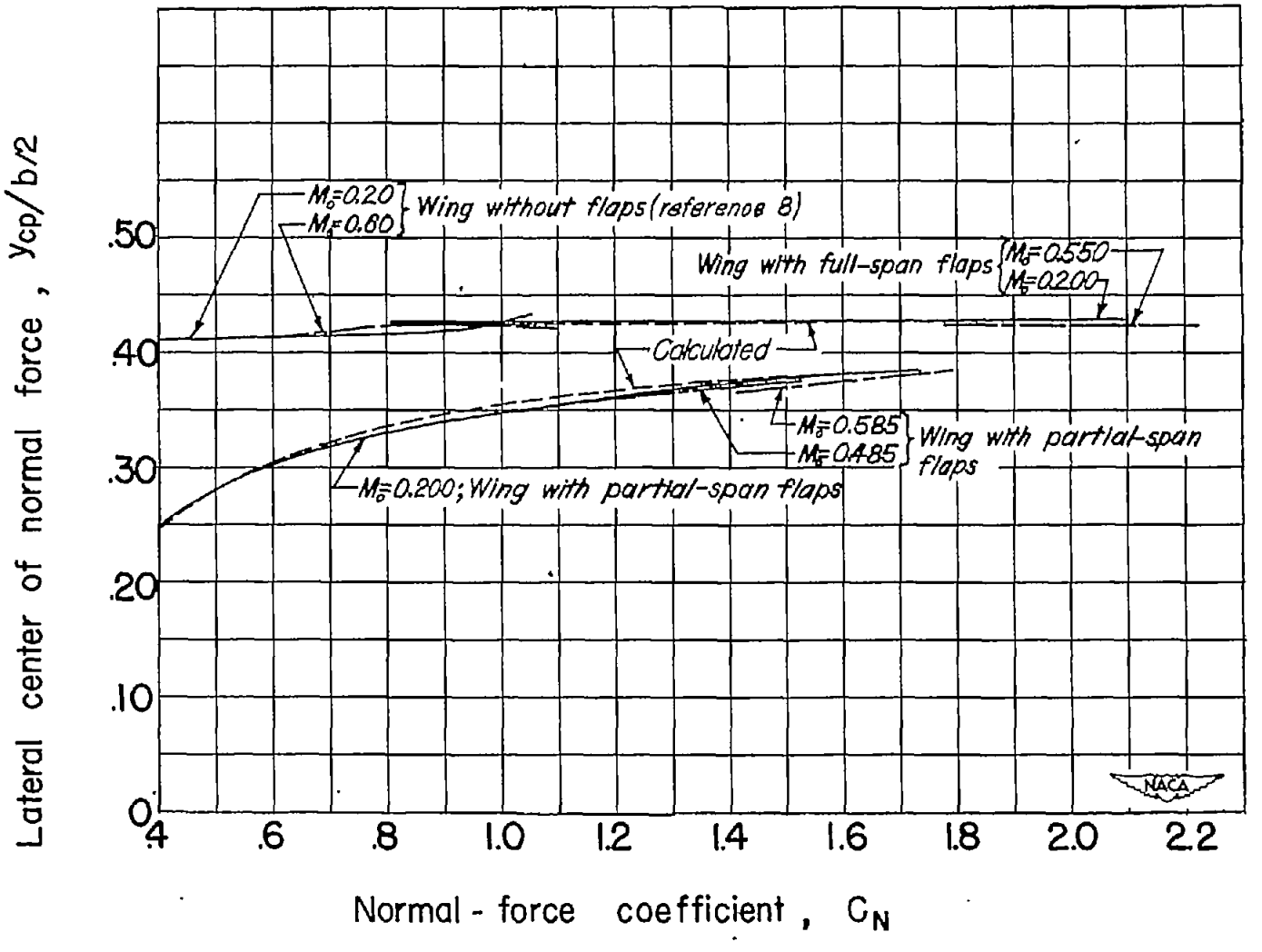

Figure 14.- Variation of lateral center of normal force with normal-force coefficient.

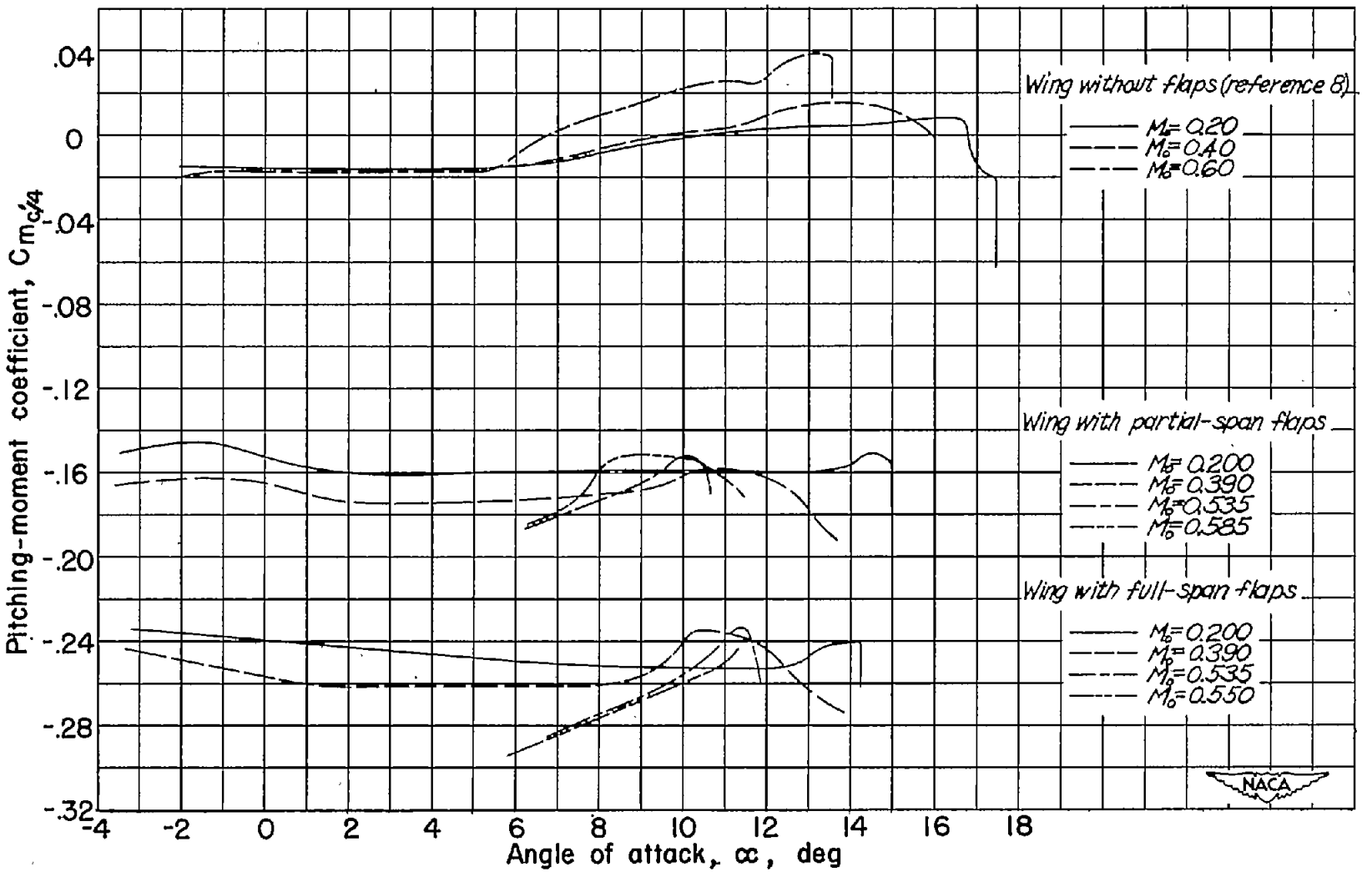

Figure 15.- Effect of Mach number on variation of pitching-moment coefficient with angle of attack.

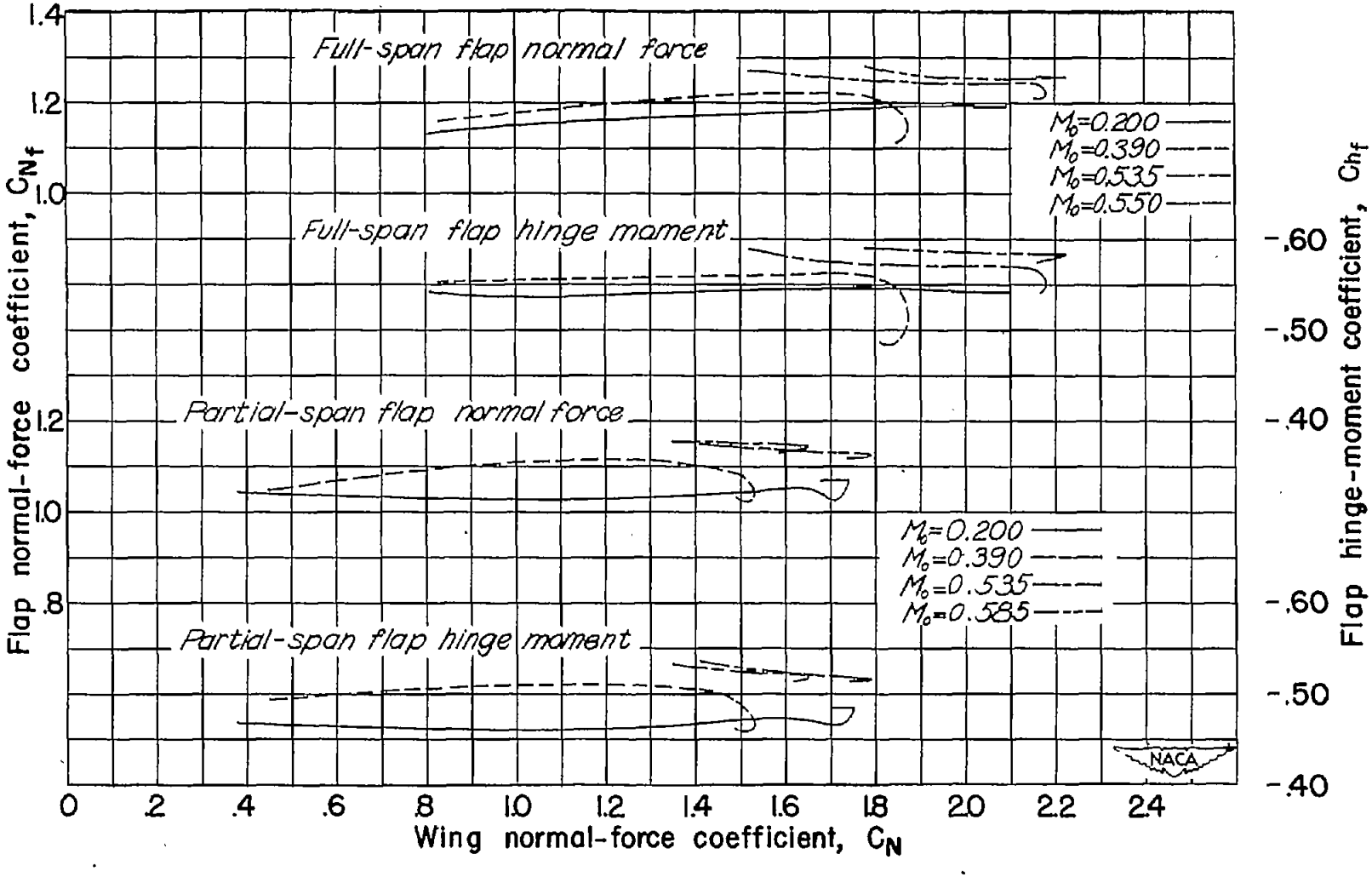

Figure 16.- Effect of Mach number on variation of flap normal-force coefficient and flap hinge-moment coefficient with wing normal-force coefficient.